energies

Review

Research Progress on Ammonia-Fueled Marine Engines

Yunkai Cai [1,2], Wenxin Gu [1,2], Bingfeng Huang [1,2] and Neng Zhu [3,*]

1 Key Laboratory of Automotive Power Train and Electronics Control, Hubei University of Automotive Technology, Shiyan 442002, China; caiyunkai@whut.edu.cn (Y.C.); 202411267@huat.edu.cn (W.G.); huangbf_qc@huat.edu.cn (B.H.)
2 School of Automotive Engineering, Hubei University of Automotive Technology, Shiyan 442002, China
3 School of Automotive and Transportation Engineering, Wuhan University of Science and Technology, Wuhan 430081, China
* Correspondence: znqc@wust.edu.cn; Tel.:+86-158-2734-5712

Abstract

Amidst the escalating global greenhouse effect, the shipping industry faces mounting pressure to decarbonize. Consequently, ammonia has emerged as a promising zero-carbon fuel for marine engines. This review systematically categorizes current research on ammonia-fueled marine engines into compression ignition (CI) and spark ignition (SI) types. CI engines, including homogeneous charge compression ignition (HCCI), partially premixed combustion (PPC), and in-cylinder high-pressure direct-injection dual-fuel (HPDF) configurations, face challenges such as limited operating ranges, difficulties in emission control (particularly NO_x and NH_3 slip), and power constraints. Conversely, SI engines encompass conventional spark plug and pre-chamber jet ignition systems. While conventional SI engines suffer from limited power output and rely heavily on reactive fuel blending, such as hydrogen, pre-chamber jet ignition shows potential to enhance combustion stability and flame speed. Despite notable progress, widespread application of ammonia fuel in marine engines is hindered by persistent technical bottlenecks, including low reactivity, slow combustion kinetics, and the formation of fuel-bound NO_x and unburned NH_3 emissions. A key unresolved technical gap is the lack of an integrated combustion–after-treatment control strategy capable of dynamically maintaining an appropriate engine-out NH_3/NO_x balance under variable marine operating conditions while simultaneously suppressing NO_x, NH_3 slip, and secondary N_2O formation, thus accelerating the practical implementation of ammonia-powered marine propulsion.

Keywords: marine engine; ammonia fuel; carbon reduction; ammonia engine; combustion mode

Academic Editor: Maria Founti

Received: 12 June 2026
Revised: 6 July 2026
Accepted: 13 July 2026
Published: 16 July 2026

1. Introduction

Fossil fuel combustion and vegetation loss are the primary drivers of rising global greenhouse gas (GHG) concentrations, thereby intensifying the greenhouse effect. Amid rapid global industrialization and economic development, this exacerbation has triggered a series of pressing environmental challenges [1]. The rise in global average temperature has caused significant glacier mass loss, subsequent sea-level rise, and a gradual reduction in habitable land area. Approximately 23% of global carbon dioxide emissions are absorbed by the oceans, increasing acidity and inflicting irreversible damage on marine ecosystems [2]. Furthermore, global warming elevates the frequency and intensity of extreme weather events—including floods, thunderstorms, wildfires, typhoons, and tsunamis—posing direct threats to human life and property [3].

Common greenhouse gases include carbon dioxide (CO_2), methane (CH_4), nitrous oxide (N_2O), hydrofluorocarbons (HFCs), perfluorocarbons (PFCs), and sulfur hexafluoride (SF_6) [4–6]. Among these, CO_2 makes the most significant contribution to the greenhouse effect. In 2021, the greenhouse effect contribution rate of CO_2 was approximately 218 times that of CH_4 (global average concentration of CH_4 is 1908 $\pm$ 2 ppb; global warming potential [GWP] = 21) [7]. It was also about 1243 times that of N_2O (global average concentration of N_2O is 334.5 $\pm$ 0.1 ppb; GWP = 290) [8]. Consequently, CO_2 remains the most critical greenhouse gas and requires focused control [9,10].

The shipping industry constitutes a significant source of GHG emissions, accounting for 1.7% of global total GHG emissions and approximately 10.5% of emissions across the entire transportation sector [11]. To reduce GHG emissions from ships, the International Maritime Organization (IMO) has put forward measures including ship energy efficiency management and power system upgrades. Among these, the adoption of low-carbon alternative fuels represents the ultimate direction for achieving long-term decarbonization goals for ships [12].

The low-carbon fuels for ships include liquefied natural gas (LNG) [13,14], methanol (CH_3OH) [15–17], ethanol (C_2H_5OH) [18], and biodiesel [19]. However, these are all carbon-based fuels with limited carbon reduction potential. Consequently, zero-carbon fuels have attracted growing attention from researchers in recent years [20]. Hydrogen (H_2) is regarded as a key fuel for reducing GHG emissions and achieving the ultimate zero-carbon economy. Nevertheless, hydrogen faces technical bottlenecks and safety risks in transportation, storage, and other related aspects [21–23]. Ammonia is considered a suitable hydrogen energy carrier. Liquid ammonia for hydrogen storage offers significant cost advantages, as ammonia can be liquefied at 0.86 MPa under atmospheric pressure or at a room temperature of 33 °C [24].

In summary, given the urgent need for carbon emission reduction in the shipping industry and the safety constraints of ships, the direct use of ammonia as a shipboard fuel offers significant advantages [25]. Det Norske Veritas (DNV) predicts that ammonia will account for 30% of the marine fuel market by 2050, while companies such as MAN Energy Solutions and Wärtsilä are actively developing and testing marine ammonia-fueled engines [26,27]. This paper summarizes the research status of ammonia engines and discusses their existing challenges and future development trends.

2. Physicochemical Characteristics, Economic Aspects, and Infrastructure for Ammonia Fuel Utilization

2.1. Production, Costs and Logistics of Ammonia Fuel

The economics of ammonia as a fuel is a complex issue, influenced by costs across multiple stages, including production, storage, transportation, and utilization. Figure 1 shows the cost and market share of green ammonia and gray ammonia. Globally, ammonia production relies mainly on natural gas and coal (in China, coal accounts for 85% of feedstock). Each ton of ammonia produced from coal emits 3.5–4.5 tons of CO_2 [28]. This conventional "gray ammonia" has low production costs. Currently, approximately 99% of global ammonia is gray ammonia, derived from fossil fuels. While its cost is relatively low, its carbon emissions are substantial [29].

In contrast, green ammonia currently has a higher production cost than conventional coal-based ammonia. Its synthesis generally relies on renewable electricity-based water electrolysis to produce green hydrogen, followed by nitrogen separation and ammonia synthesis. Therefore, the renewable electricity price is a key factor determining the cost of green ammonia. In China, when the renewable electricity price is in the range of 0.15–0.3 CNY/kWh, the production cost of green ammonia has been estimated at approximately 2920–4600 CNY per ton, which is about 1.2–2.1 times that of coal-based ammonia. By comparison, when the coal price is 700–900 CNY per ton, the production cost of coal-based ammonia is approximately 2200–2500 CNY per ton. With further reductions in renewable electricity costs and improvements in electrolyzer efficiency, the cost of green ammonia is expected to decrease substantially in the future [30]. Whether used in direct combustion or fuel cells, ammonia fuel currently has a higher cost than conventional fossil fuels. For example, the fuel cost of ammonia-fueled ships is approximately 1.5–2 times that of diesel-powered vessels [31].

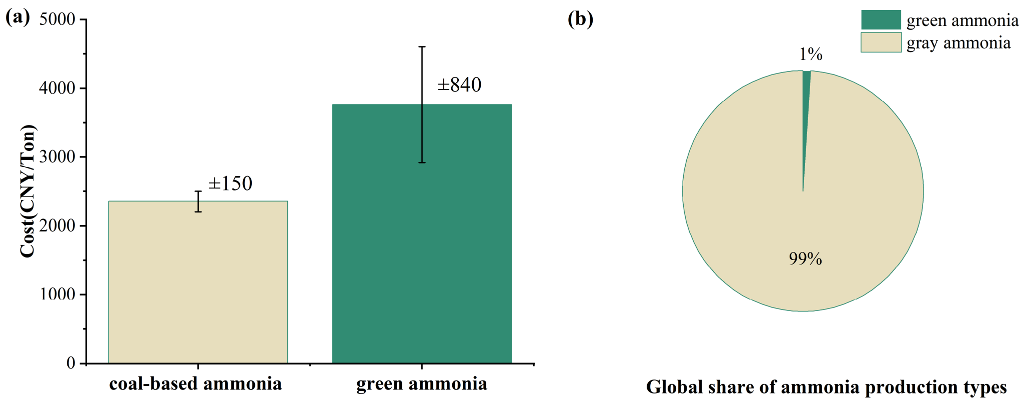

Figure 1. The cost and market share of green ammonia and gray ammonia. (**a**) Production cost of coal-based gray ammonia and green ammonia; (**b**) Global market share of different ammonia production routes.

However, with the decline in renewable energy costs, the maturation of green ammonia production technologies, and the scaling up of production, the cost of ammonia fuel is expected to decrease. It is anticipated that, after 2030, the cost of green ammonia may become comparable to that of conventional fuels, with particularly high application potential in shipping, industrial boilers, and other sectors [32].

In terms of storage and transportation, ammonia can leverage existing liquefied gas cylinders and pipeline networks. The density of liquid ammonia is comparable to that of gasoline, making it well suited for long-distance transport. Therefore, ammonia offers notable convenience as a marine fuel in terms of storage and logistics. However, its corrosiveness (which affects metals such as copper and zinc) and toxicity (with a threshold limit value, TLV, of 25–50 ppm) require careful consideration.

2.2. Physical–Chemical Characteristics, Combustion Limitations and Technical Solutions of Ammonia Fuel

Table 1 presents the physicochemical properties of ammonia and conventional fuels. Ammonia (NH_3) is a polar molecule with a trigonal pyramidal structure, consisting of one nitrogen atom and three hydrogen atoms. Since it contains no carbon element, it does not emit CO_2, CO, or soot particles under ideal complete combustion conditions, and is thus recognized as a zero-carbon fuel with considerable carbon reduction potential [33]. In terms of physical properties, ammonia has a relatively low boiling point (−33.3 °C) and can be liquefied under moderate pressure at room temperature. The volumetric energy density of liquid ammonia is approximately 11.3 GJ·m^{-3}, which is higher than that of compressed hydrogen and comparable to that of liquefied natural gas (approximately 14.7 GJ·m^{-3}). This allows ammonia to be stored on a large scale and transported over long distances using the existing, well-established chemical infrastructure, an advantage that is particularly notable in engineering applications [34].

Table 1. Physicochemical properties of ammonia and traditional fuels [34–36].

Physicochemical Properties	NH_3	Natural Gas	H_2	Diesel	Gasoline
Boiling point (K)	239.6	111	20.2	453–644	298–483
Energy density (MJ/m^3)	11,333	7132	8539	36,403	31,047
Lower heating value (MJ/kg)	18.6	48.28	119.6	42.5	44.5
Autoignition temperature (k)	~924	723	844	503	723
Flammability limits (%)	15–27	5–13.9	4.7–75	0.6–6.5	0.6–8
Minimum ignition energy, MJ	8	0.28	0.02	N/A	0.24
Octane number (RON)	130	107	≥100	15–25	90–98
Cetane number	N/A	N/A	N/A	40–55	13–17
Laminar flame velocity (cm/s@300 K, 1 bar)	7	37	291	30	43
Latent heat of vaporization (kJ/kg)	1370	N/A	455	250	348.7
Freezing point/melting point (K)	195.4	90.7	14.0	Grade-dependent	Mixture-dependent
Liquid density ($kg \cdot m^{-3}$)	682	422	70.5	830–850	720–760
Gaseous density ($kg \cdot m^{-3}$)	0.729	0.680	0.085	N/A	N/A

By contrast, in terms of combustion and chemical characteristics, ammonia exhibits properties markedly different from those of conventional hydrocarbon fuels. Its lower heating value is only approximately 18.6 $MJ \cdot kg^{-1}$, the autoignition temperature is as high as ~924 K, the minimum ignition energy is substantial, the flammability limits are narrow (around 15–27%), and the laminar flame propagation speed is extremely low [35]. These characteristics give rise to challenges such as difficult ignition, slow combustion rates, and insufficient combustion stability when ammonia is utilized in internal combustion engines. Meanwhile, the nitrogen contained in ammonia molecules inevitably leads to the formation of fuel-bound NO_x during combustion, and under incomplete combustion conditions, unburned ammonia emissions may also occur, posing more stringent challenges for engine emission control. In addition, liquid ammonia has a high latent heat of vaporization and high saturated vapor pressure. During high-pressure injection, it is prone to flash boiling and transcritical phase transitions, which complicate the in-cylinder processes of spray, evaporation, and mixing [36].

As a result, conventional injection and combustion control strategies developed for diesel or gasoline engines cannot be directly applied. Overall, ammonia as a fuel boasts several distinct advantages, including its zero-carbon attribute, favorable storage and transportation characteristics, and relatively high volumetric energy density. However, its inherently low reactivity and slow combustion kinetics, as well as the issues of NO_x and unburned ammonia emissions, have become key technical bottlenecks restricting its application as a fuel for internal combustion engines. Therefore, practical engineering applications usually require synergistic optimization through measures such as dual-fuel combustion, hydrogen enrichment, advanced injection strategies, and exhaust after-treatment technologies.

For marine applications, however, hydrogen enrichment should not be regarded as a simple plug-in solution. Although hydrogen can effectively compensate for the low reactivity and slow flame speed of ammonia, its onboard supply remains a critical engineering constraint. Direct storage of compressed or liquefied hydrogen requires additional tanks, safety barriers, ventilation systems, leak detection and explosion-prevention measures, which may reduce the volumetric advantage of ammonia as a marine fuel. An alternative approach is onboard ammonia cracking, in which part of the stored ammonia is decomposed into a hydrogen–nitrogen mixture and then supplied to the engine as an ignition promoter or combustion enhancer. This strategy avoids carrying a separate hydrogen fuel, but introduces new challenges related to catalyst durability, cracking efficiency, heat management, transient response and system integration with engine load variations. In particular, exhaust-heat-driven cracking may improve overall energy utilization, but its hydrogen production rate may not always match the rapid load changes in marine engines. Therefore, future hydrogen-assisted ammonia engines should be evaluated not only by combustion performance, but also by onboard hydrogen sourcing, storage safety, cracking efficiency and control complexity.

3. The Origin of Ammonia Engines

In the 1940s, the Second World War caused a sharp decline in oil resources, and ammonia became one of the alternative fuels for internal combustion engines [37]. In 1945, Kroch first realized the use of liquid ammonia as automotive fuel and gas as the ignition agent for ammonia, which performs equally well in terms of power and economy as gasoline engines [38]. The feasibility of the pure ammonia engine was proposed. In the 1960s, driven by new environmental legislation and energy crises, ammonia engines with ignition systems were proven to be feasible for military applications. Related studies have shown that using 4–5% of the total fuel mass of hydrogen to ignite ammonia can effectively improve engine performance [39–41]. For engines that only use ammonia as fuel, higher compression ratios or spark plugs with higher ignition energies are required to achieve normal combustion in the cylinder. In addition, the feasibility of the dual-fuel scheme using diesel as the ignition agent has been verified [42,43].

In recent years, environmental protection, energy conservation, and emission reduction have become a global consensus. As a zero-carbon fuel and clean energy source, ammonia has attracted widespread attention. Efficient combustion strategies for engines, such as homogeneous charge compression ignition (HCCI), partially premixed combustion (PPC), and low-temperature combustion (LTC), have all made significant progress [44,45]. Advanced engine clean combustion technology and electronic control technology provide technical support and create new ideas for the development of ammonia engines. The development process of the ammonia engine is shown in Figure 2.

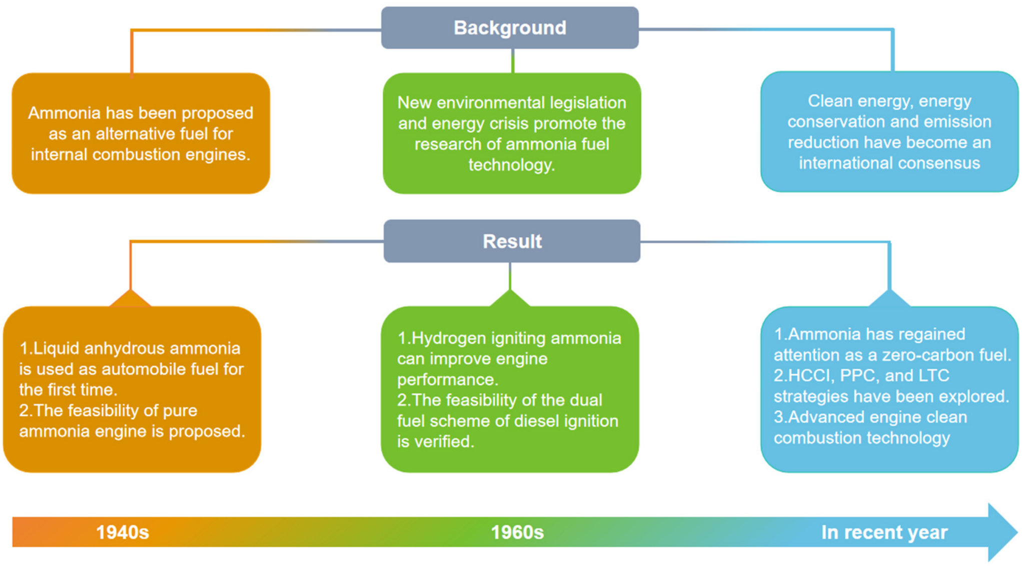

Figure 2. Timeline of ammonia engine development.

4. Marine Compression Ignition Ammonia Engines

4.1. Marine HCCI Ammonia Engines

The HCCI ammonia engine draws in a homogeneous ammonia–hydrogen mixture. As shown in Figure 3, during the compression stroke, the mixture autoignites. This combustion mode features uniform combustion, a low peak temperature, and low emissions, combining the high efficiency of diesel engines with the low emissions of premixed gasoline combustion. However, ammonia has low chemical reactivity, a high autoignition temperature, long ignition delay, and narrow autoignition limits, which make combustion phasing and stable autoignition difficult to control in the HCCI operation.

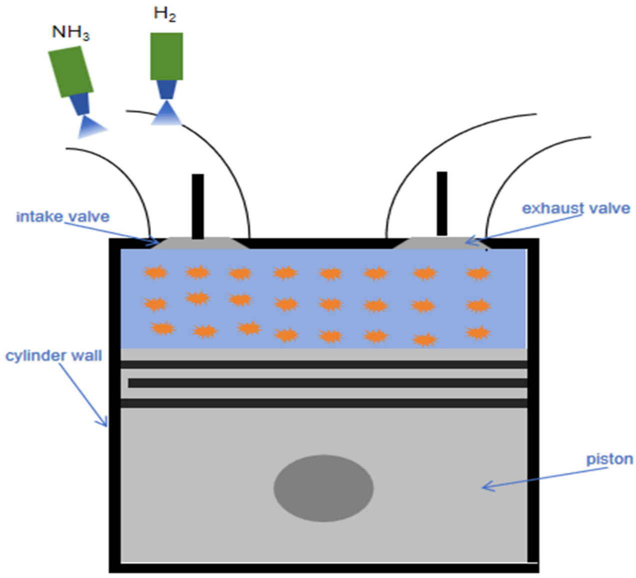

Figure 3. HCCI ammonia engine's working schematic diagram.

In terms of combustion stability and ignition, the increasing ammonia fraction reduces stability and extends ignition delay. Pochet et al. [46,47] found that, at 70% ammonia fraction, higher intake pressure and temperature are needed for stable combustion. A higher ammonia fraction increases the risk of misfire, but it can moderate the excessively rapid heat release associated with pure hydrogen operation, thereby reducing the tendency toward excessive pressure rise. As reported by Wang et al. [48], relevant parameter tests yielded the following results: At a compression ratio of 19 and an excess air ratio of 3.0, hydrogen addition or nitrogen replacement by argon reduced the ignition delay from 700 ms to 0.31 ms, increased the heat conversion efficiency from 65.1% to 78.2%, and increased the power density by 20%. Yan et al. [49] noted that the pure ammonia HCCI operation may suffer from misfire under certain conditions, while hydrogen addition can improve start-up performance and promote autoignition. However, excessive hydrogen addition may result in overly rapid heat release and an excessive pressure rise rate, thereby narrowing the stable operating range of ammonia HCCI engines. Overall, combustion stability is affected by ammonia fraction, compression ratio, intake temperature, and hydrogen addition, with an optimal balance of about 20% hydrogen and an equivalence ratio of 0.3 for non-road applications.

Regarding emissions, NO_x from ammonia-fueled HCCI engines is mainly influenced by ammonia fraction and combustion temperature. Pochet et al. [46] found that increasing ammonia fraction raises NO_x from 6 ppm to 1000–3500 ppm. Exhaust gas recirculation (EGR) can reduce NO_x but lowers cylinder temperature and combustion efficiency. Yan et al. [49] emphasized that high ammonia fractions increase fuel-based NO_x. Under lean combustion conditions, there is a trade-off between ignition delay, thermal efficiency, and NO_x, requiring the careful control of ammonia fraction, hydrogen addition, EGR, and inert gas dilution.

Figure 4 shows the working characteristics of an HCCI ammonia engine. Hydrogen acts as an ignition promoter and a combustion enhancer in ammonia-fueled HCCI engines, improving combustion reactivity, shortening ignition delay, and expanding operating range. However, excessive hydrogen leads to an overly rapid heat release rate and a high pressure rise rate, which in turn narrows the stable operating range of homogeneous charge compression ignition (HCCI) [50]. Therefore, controlling the hydrogen fraction at approximately 20% is appropriate, and this ratio is suitable for off-road applications or medium-to-low load operating conditions. HCCI ammonia engines have a narrow operating range (900–1800 rpm), limiting adaptability to complex marine conditions. Because ammonia HCCI combustion is highly sensitive to mixture temperature and compression conditions, stable operation often requires the careful control of the compression ratio, intake temperature, hydrogen fraction, heat release rate, and pressure rise rate. These control strategies can help reduce NO_x emissions, but they may also lower combustion efficiency, increase CO emissions, and shift the combustion phasing. Hydrogen addition improves combustion stability and expands the operating range of ammonia HCCI engines. However, for marine applications, the benefit of hydrogen must be balanced against onboard storage volume, leakage risk, ammonia-cracking efficiency and transient control complexity. Therefore, hydrogen-assisted HCCI should be considered a system-level solution rather than only a combustion-enhancement strategy.

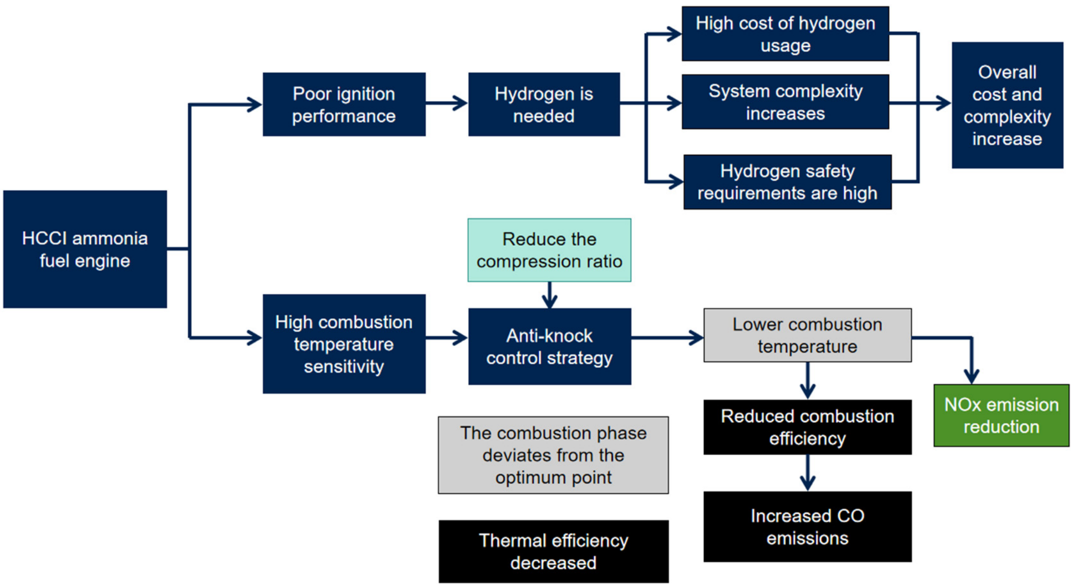

Figure 4. Working characteristics of HCCI ammonia engine.

4.2. Marine PPC Ammonia Engine

Due to the high reactivity of fuel, it is difficult to control combustion phasing and the heat release rate, which leads to rough combustion and limits the applicable load range of the HCCI combustion mode [51,52]. Studies have shown that fuels with a high research octane number (RON) exhibit strong autoignition resistance, which can help moderate the heat release rate, reduce excessive pressure rise, and improve engine thermal efficiency in PPC. Through in-depth research by numerous domestic and foreign scholars, a new combustion mode named partially premixed combustion (PPC) has been proposed based on the HCCI mode. This mode expands the load range for efficient and clean combustion in compression ignition engines [53,54]. In addition, PPC requires fewer modifications to traditional compression ignition engines. Therefore, in recent years, numerous studies have been conducted on partially premixed compression ignition by injecting ammonia into the intake port, with diesel engines, dimethyl ether engines and other compression ignition engines as the prototype machines.

The emission characteristics of ammonia-fueled engines are affected by the ammonia blending ratio, load conditions, and combustion mode. Reiter and Kong reported that NO_x emissions tend to decrease when the ammonia energy ratio is below 40%. However, when the ratio exceeds 40%, NO_x emissions begin to rise, while CO and HC emissions increase and CO_2 emissions decrease [55,56]. Gill compared the combustion performance of pure ammonia and dissociated ammonia (H_2 + N_2 + a small amount of NH_3) under high-load conditions. The results show that pure ammonia offers better combustion stability and thermal efficiency, but NO_x emissions increase, accompanied by N_2O formation [57]. Gross investigated an ammonia/DME direct-injection engine (as schematically illustrated in Figure 5) and found that ammonia addition prolongs ignition delay and reduces engine load capacity. Meanwhile, emissions of CO, HC, and fuel-bound NO_x increase [58]. Niki further found that increasing ammonia injection quantity lowers the maximum in-cylinder pressure and delays ignition timing. NH_3 and N_2O emissions increase, while CO_2 emissions decrease [59,60]. Yousefi demonstrated that using split diesel injection can reduce unburned ammonia emissions, achieving a reduction of approximately 83.5% compared with single injection. Meanwhile, the indicated thermal efficiency in dual-fuel mode can be increased by about 2%, and greenhouse gas emissions are reduced by 23.7% [61,62]. Overall, ammonia co-combustion can reduce CO_2 emissions, but it leads to increased NO_x and NH_3 emissions. Therefore, emission control remains a key challenge for ammonia-fueled engines.

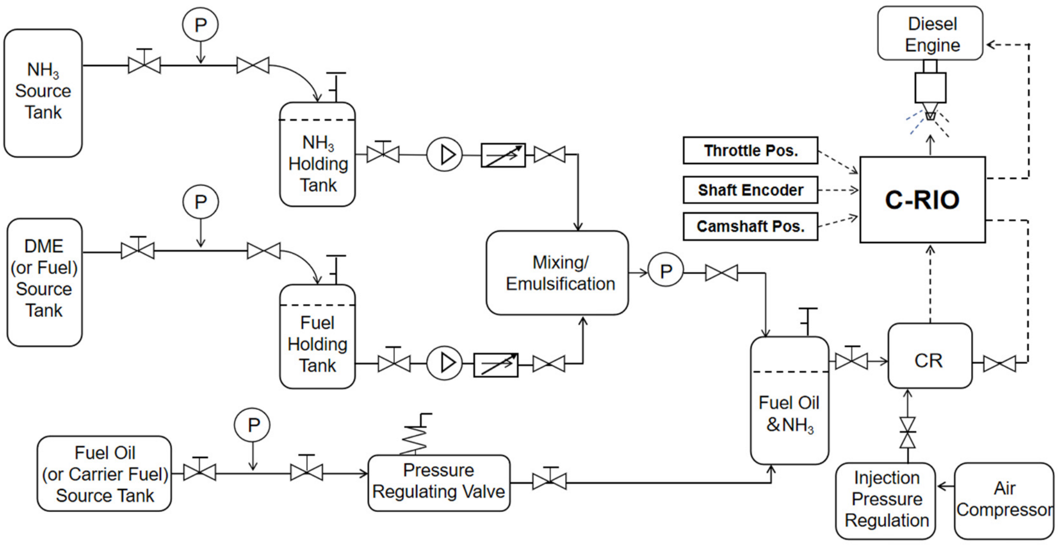

Figure 5. Fuel flow diagram for preparation and delivery of ammonia and DME mixtures. (Solid arrowed lines: fluid pipelines and flow directions; dashed arrowed lines: electrical, measurement, control and feedback signals. Horizontal dashed line in storage tank: rated liquid level. Circles labeled "P": pressure measuring points; bowtie symbols: shut-off/control valves; circles with internal triangles: transfer pumps).

Regarding engine power and thermal efficiency, several studies have shown that adjusting the blending ratio of ammonia to diesel (or other auxiliary fuels) can optimize engine power output and thermal efficiency. Reiter and Kong [55,56] conducted research on an ammonia/diesel dual-fuel (ADDF) PPC engine. Their results demonstrate that the ammonia energy ratio can reach up to 95%. Increasing the ammonia ratio enables the engine to achieve power output exceeding the rated power of pure diesel mode, and the engine can maintain favorable fuel economy at a specific ammonia ratio under constant power conditions. Nadimi [63] investigated an ammonia/biodiesel dual-fuel engine, in which the engine was first operated stably on biodiesel under low-load conditions with a constant biodiesel mass flow rate. Ammonia was then injected to increase engine torque

https://doi.org/10.3390/en19143357

and power output (as illustrated in Figure 6). The results indicated that stable operation could be achieved when ammonia supplied approximately 69.4% of the total energy input, although thermal efficiency slightly decreased. These studies indicate that ammonia co-combustion can enhance the engine's power potential, but a balance must be struck between the ammonia ratio and thermal efficiency.

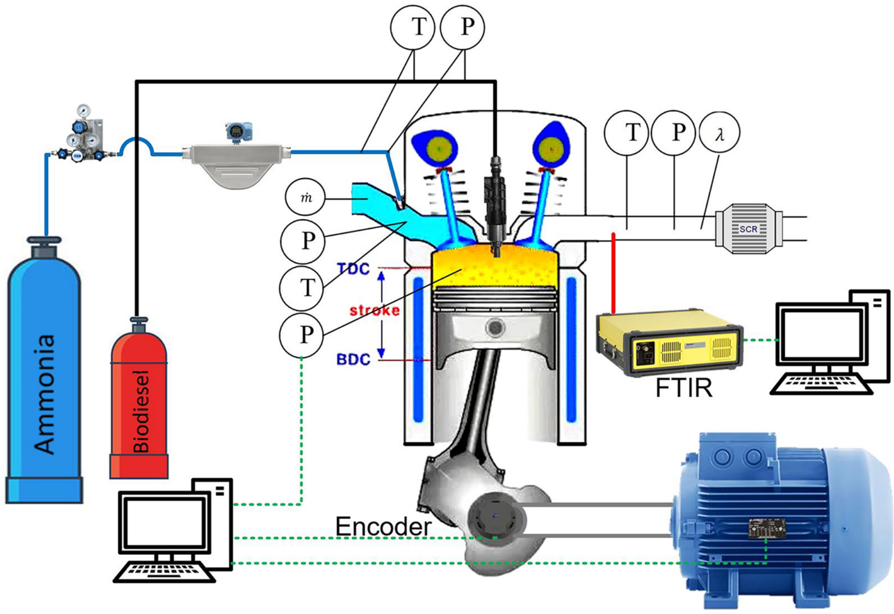

Figure 6. Experimental schematic diagram of amino biodiesel dual-fuel engine. P and T represent the pressure and temperature measurement points, respectively. Reproduced with permission from ref. [63]. Copyright 2022 WILEY.

Injection strategy has a significant impact on engine performance and emissions. Studies have shown that multiple injections and advanced diesel injection timing can effectively control combustion phasing, while also improving NH_3 and N_2O emissions under high-load conditions and maintaining high thermal efficiency [64]. Lasocki and Kane proposed using engine waste heat to partially decompose ammonia, which enhances mixture uniformity and helps reduce unburned ammonia and NO_x emissions [65–67]. Yousefi further confirmed through experiments and simulations that split injection can reduce unburned ammonia and improve thermal efficiency; however, after-treatment technology is still required to bring NH_3 emissions into compliance [61,62].

Regarding the potential application of ammonia in low-speed two-stroke marine engines, Liu [68] developed an ammonia engine model and evaluated its performance and emissions. The results indicate that ammonia can meet the compliance requirements and thermal efficiency benchmarks of typical marine engines, whether supplied in the liquid or gaseous form. Liquid ammonia supply outperforms gaseous ammonia in terms of power output, ammonia slip, and thermal efficiency. Additionally, CO_2 and CO emissions are reduced, and NO_x emissions meet the Tier II standard. Table 2 shows the emission performance of the PPC engine.

The above literature indicates that co-combustion with ammonia is beneficial for reducing CO_2 emissions. However, it also leads to challenges related to NO_x, ammonia slip, and, in some cases, N_2O emissions. The ammonia energy fraction is a key factor affecting emissions. When the ammonia energy ratio is below approximately 40%, NO_x emissions decrease. When the ratio increases further, NO_x, CO, and HC emissions tend to rise, while CO_2 emissions continue to decrease. In addition, combustion mode, engine load, and injection strategy have significant effects on emissions. Multiple and split injection strategies can effectively reduce unburned ammonia and improve combustion stability. Nevertheless, after-treatment systems are still required to meet emission regulations.

Table 2. Emission performance of PPC engine. (Note: ↑ = increased emission concentration; ↓ = reduced emission concentration).

Authors	Fuel Situation	Measure	Emission Characteristics
Reiter and Kong [55,56]	Ammonia/diesel	Mixing ammonia gas	CO and HC ↑; CO_2 ↓; NO_x ↓
Gill et al. [57]	Pure ammonia and dissociated ammonia	Comparison of pure ammonia and dissociated ammonia	Pure ammonia NO_x emissions increase
Gross et al. [58]	Ammonia/dimethyl ether	Compression ignition of DME to ignite ammonia	CO and HC ↑; NO_x ↑ due to fuel-bound nitrogen; NH_3 slip: several hundred ppm; soot extremely low
Niki et al. [59]	Ammonia/diesel	Spray ammonia gas to the intake pipe	Mixing ammonia gas: NH_3, H_2O, and N_2O ↑; CO_2 linearly ↓
Niki et al. [60]	Ammonia/diesel	Multi-stage ammonia injection	NH_3 and N_2O ↓; in some cases, N_2O ↑
Kane et al. [66,67]	Ammonia/diesel	Compare the concentration of emissions before and after the device	Proper catalyst selection enabled simultaneous reduction of NO_x and NH_3
Nadimi et al. [63]	Ammonia/biodiesel dual fuel	Mixing ammonia gas	CO_2, CO, and HC ↓; NO ↑
Yousefi et al. [61]	Ammonia/diesel	Various injection timings	Ammonia energy fraction < 40%; NO_x ↓ 58.8%; N_2O ↑
Yousefi et al. [62]	Ammonia/diesel	Multi-injection strategies	NH_3 ↓ 83.5%; minimum NH_3 slip ≈ 900 ppm

Overall, ammonia co-firing in compression ignition engines has significant potential for carbon reduction and power enhancement. However, large-scale application is still limited by the control of NO_x, NH_3, and N_2O emissions. Future studies should focus on the coordinated optimization of combustion modes, injection strategies, and efficient after-treatment technologies to achieve the best balance between performance and emissions. It should be noted that many PPC ammonia studies reviewed in this section were conducted on automotive-scale diesel engines, single-cylinder research engines or laboratory platforms rather than low-speed two-stroke marine engines. These studies are still valuable because they reveal fundamental mechanisms, including the effects of ammonia energy fraction, pilot-fuel timing, split injection and mixture stratification on ignition delay, NO_x formation, NH_3 slip and N_2O emissions. However, their direct transferability to large low-speed marine engines is limited. Marine two-stroke engines differ substantially in bore size, engine speed, scavenging process, in-cylinder flow structure, spray penetration distance, wall heat transfer and continuous high-load operating requirements. Therefore, the results from automotive or research engines should be interpreted as mechanistic evidence for ammonia combustion control rather than direct proof of marine-engine readiness. Further validation on large-bore, low-speed two-stroke platforms is required before PPC ammonia combustion can be considered technically mature for main marine propulsion.

5. Marine Mixed Thermodynamic Cycles and Ammonia Dual-Fuel Engines

In addition to HCCI, PPC, and spark ignition ammonia engines, some ammonia-fueled marine engines operate under mixed thermodynamic-cycle and dual-fuel combustion modes. In these engines, the heat release process cannot be strictly classified as purely Otto-like or Diesel-like, because pilot-fuel autoignition, ammonia injection, partially premixed combustion, and mixing-controlled combustion may coexist within the same engine cycle. Therefore, these engines should be discussed separately from conventional compression ignition and spark ignition ammonia engines.

This classification is particularly relevant to ammonia/diesel dual-fuel engines. In low-pressure or intake-premixed ammonia systems, ammonia is supplied through the intake port or manifold and ignited by a small amount of high-reactivity pilot fuel. Although this approach can reduce CO_2 emissions, gaseous ammonia may displace part of the intake air and reduce power density, while ammonia's low reactivity can also lead to incomplete combustion and high NH_3 slip. To overcome these limitations, high-pressure direct-injection dual-fuel (HPDF) ammonia engines have attracted increasing attention. In the HPDF operation, ammonia is injected directly into the cylinder at high pressure and ignited by a diesel pilot, which can better preserve charging efficiency, improve spray–air mixing, and provide more direct control over combustion phasing and emissions [69].

In recent years, high-pressure injection dual-fuel (HPDF) engines have been considered to have the potential to reduce emissions and improve thermal efficiency [70–72]. The HPDF ammonia engine uses a small amount of highly reactive fuel (such as diesel) as an ignition source to assist in igniting the hard-to-autoignite ammonia fuel, thereby achieving an efficient and low-carbon combustion process. The HPDF ammonia engine draws in a mixture of ammonia and hydrogen during the intake stroke. In the compression stroke, the piston compresses the mixture, raising its temperature and pressure. During the power stroke, the diesel injector sprays diesel into the cylinder. The diesel autoignites and then ignites the ammonia–hydrogen mixture. The released energy pushes the piston downward, producing mechanical work. Finally, during the exhaust stroke, the combustion gases are expelled (as shown in Figure 7).

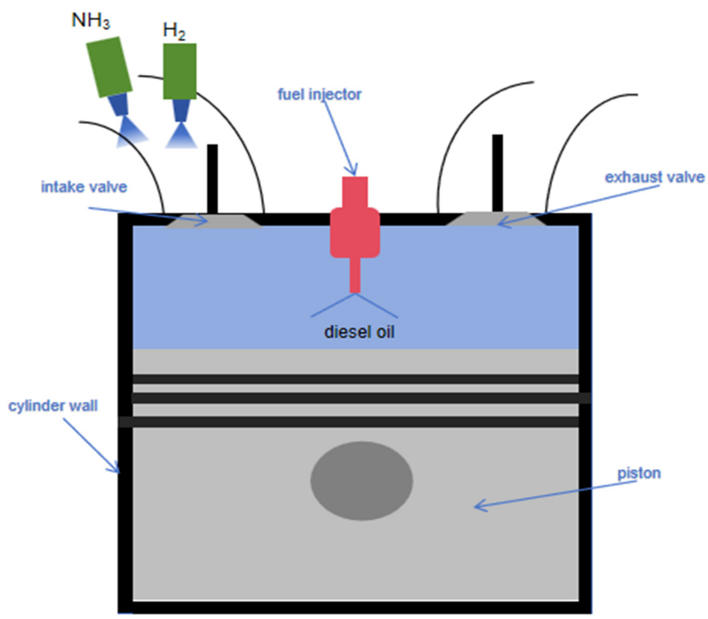

Figure 7. Working diagram of HPDF ammonia engine.

In 2021, Frankl et al. [73,74] carried out relevant numerical simulation research on an HPDF ammonia fuel engine, which provided theoretical guidance for the research in this direction. Li et al. [75] carried out experimental research and numerical simulations on an HPDF ammonia/diesel dual-fuel engine. They focused on the combustion and emission characteristics of low- and high-pressure injection dual-fuel modes. The results show that the maximum ammonia energy recommended by the low-pressure injection mode accounts for about 80%, while the high-pressure injection has the potential to achieve a 97% diesel substitution rate. The HPDF ammonia/diesel mode has similar indicated thermal efficiency, cooling and exhaust loss to the pure diesel mode. Low-pressure injection can obtain higher indicated thermal efficiency. Compared with the LPDF mode with 20% diesel energy fraction, the HPDF mode with 3% diesel energy fraction reduced NH_3 by approximately 80–85%, NO_x by 65–75%, and equivalent CO_2 emissions by 80–85% under the same 1000 rpm, $-8°$CA aTDC, 1.3 bar and 322 K operating condition.

In terms of emission performance, Sun et al. [76] explored the effects of different ignition modes and different injector arrangements on the performance of HPDF ammonia/diesel dual-fuel engines. The results show that the combustion performance of the HPDF-1 arrangement is more stable than that of the HPDF-2 arrangement, which is due to the fact that the injector arrangement is beneficial to the rapid mixing of fuel, thus promoting the combustion process. In addition, compared with the hydrogen-induced ammonia ignition mode, the ammonia/hydrogen mixed compression ignition mode reduces the nitrogen oxide emissions by 29.4%, with a 0.7% decrease in the indicated power. When the ammonia/hydrogen mixing ratio is 30%, it is close to the original engine emission, and the ammonia and hydrogen escape decreases with the increase in the mixing ratio.

These results indicate that injector arrangement and ignition mode are important control factors in HPDF ammonia engines. A suitable injector layout can improve the spatial matching between the ammonia jet and the ignition region, thereby promoting fuel–air mixing and reducing unburned NH_3/H_2 slip. However, ignition strategies with stronger hydrogen participation may increase power output while also raising NO_x emissions. Therefore, the injector arrangement, ignition mode and ammonia/hydrogen mixing ratio should be optimized together to balance combustion stability, power performance and emission control.

In terms of engine power, Wang et al. [77] investigated the effects of different ammonia/hydrogen mixing ratios on engine combustion and emission performance at four intake temperatures ranging from 476 K to 551 K. They found that, under the hydrogen ignition mode at an intake temperature of 476 K, a 30% hydrogen mixing ratio resulted in higher engine power, better emission performance, a KI value slightly above 2 MPa/°CA, fewer components performing negative work, and overall optimal engine performance.

In addition to the above studies, recent research has further confirmed the potential of liquid ammonia high-pressure direct injection and diesel pilot ignition for marine and heavy-duty engines. Scharl et al. [78] investigated the ignition and combustion characteristics of diesel-piloted liquid ammonia sprays under engine-relevant conditions using a rapid compression–expansion machine. Their results showed that successful ammonia spray combustion strongly depends on the spatial and temporal interaction between the diesel pilot spray and the liquid ammonia spray. This indicates that, for HPDF ammonia engines, the relative arrangement of diesel and ammonia injection is not only a hardware issue, but also a key factor controlling ignition stability, heat release and unburned ammonia emissions.

Zhou et al. [79] established the CFD models of a pilot diesel-ignited ammonia dual-fuel low-speed marine engine and compared ammonia premixed combustion with high-pressure spray combustion. The results showed that both modes could achieve an indicated thermal efficiency above 50% at a diesel replacement ratio of approximately 98–99%. However, the optimized premixed mode increased NO_x emissions by 140.6% compared with the pure diesel mode, whereas the optimized high-pressure spray combustion mode reduced NO_x emissions by about 47%. In both optimized cases, the equivalent greenhouse gas emissions, expressed as $CO_2 + 300 \times N_2O$, were reduced by approximately 97%, and unburned NH_3 emissions were negligible. These results suggest that HPDF ammonia combustion has stronger potential for simultaneous carbon reduction and emission control in low-speed marine engines.

Zhang et al. [80] experimentally investigated an ammonia/diesel dual direct-injection strategy on a two-stroke low-speed compression ignition engine based on the diesel jet-controlled compression ignition concept. They found that diesel spray can provide sufficient ignition energy for liquid ammonia spray, thereby shortening the ammonia combustion duration and improving the indicated thermal efficiency compared with pure diesel operation. Meanwhile, soot, CO and thermal NO_x emissions were effectively suppressed under the dual-fuel mode. This study is particularly important for marine applications because it directly verifies the feasibility of liquid ammonia direct injection in a two-stroke low-speed engine rather than only in automotive-scale research engines.

These studies also show that diesel pilot fuel plays a critical but conflicting role in HPDF ammonia engines. Increasing the pilot-fuel quantity can strengthen ignition, shorten ammonia combustion duration and improve combustion stability, but it also weakens the carbon-reduction benefit of ammonia substitution. Conversely, reducing the pilot-fuel quantity helps lower fossil CO_2 emissions, but may increase ignition delay, unstable combustion and NH_3 slip. Therefore, the practical target is not to eliminate pilot fuel completely, but to find an operating window that balances ammonia substitution, ignition stability, thermal efficiency and emissions.

Overall, HPDF ammonia engines provide a more promising mixed-cycle pathway for large marine propulsion than low-pressure or intake-premixed ammonia dual-fuel systems. By injecting ammonia directly into the cylinder and using a small amount of diesel pilot fuel for ignition, the HPDF operation can preserve charging efficiency, maintain power density, and achieve high ammonia substitution while improving combustion controllability. However, HPDF ammonia combustion still involves important trade-offs. Increasing the pilot-fuel quantity can improve ignition stability and reduce NH_3 slip, but it also weakens the carbon-reduction benefit. Reducing the pilot-fuel quantity can increase the zero-carbon fuel share, but may cause unstable ignition, incomplete ammonia oxidation, and higher NH_3 slip. Similarly, ammonia injection pressure, injector arrangement, and spray–pilot interaction strongly affect NO_x formation, NH_3 slip, thermal efficiency, and combustion stability.

Therefore, the key challenge for HPDF ammonia engines is to establish a controllable operating window that coordinates ammonia injection pressure, pilot-fuel strategy, injector layout, combustion phasing, and exhaust after-treatment. For large marine engines, future research should focus on validating HPDF ammonia combustion under large-bore, low-speed, high-load, and transient operating conditions, while coupling in-cylinder combustion optimization with SCR/ASC after-treatment to achieve high efficiency, low NO_x, low NH_3 slip, and low residual carbon emissions.

6. Marine Spark Ignition Ammonia-Fueled Engine

6.1. Marine Conventional Spark Ignition Ammonia Engine

The conventional spark ignition ammonia engine is a combustion mode of an internal combustion engine based on the spark ignition principle of gasoline engines, using ammonia (NH_3) as the main fuel. Due to the high autoignition temperature and low combustion rate of ammonia, this type of engine usually requires spark plug ignition and is often supplemented with hydrogen or other easily combustible fuels to improve combustion performance.

During the intake stroke, the engine intake valve opens, drawing in a mixture of ammonia and hydrogen. In the compression stroke, the intake valve closes, and the piston moves upward, compressing the mixture and raising its temperature and pressure. During the power stroke, the spark plug ignites the ammonia–hydrogen mixture. The released energy pushes the piston downward, producing mechanical work. In the exhaust stroke, the exhaust valve opens, and the piston moves upward to expel the combustion gases, completing one cycle (as shown in Figure 8).

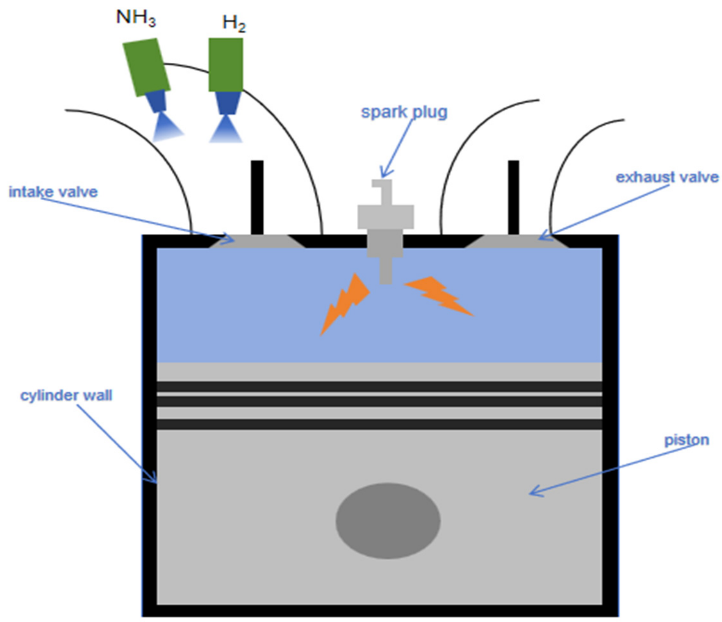

Figure 8. Working diagram of conventional ignition ammonia engine.

It is generally believed that pure ammonia can be ignited with at least 8 mJ ignition energy [81]. The spark plug is used to ignite ammonia gas in the engine cylinder. Due to the slow combustion rate of ammonia gas, single-point ignition reduces the pressure rise rate, and the combustion duration is longer. This makes the engine use a spark plug to ignite ammonia gas in the cylinder. Therefore, the ignited ammonia-fueled engine generally blends other highly active fuels with a faster flame propagation speed. The blended fuels in the existing research are mainly hydrogen, gasoline and natural gas.

Many studies have focused on the ignition behavior, flame propagation speed, and cycle stability of ammonia or ammonia–hydrogen mixtures in spark ignition engines. Mørch et al. [82] mixed ammonia and hydrogen in the intake port and varied the excess-air ratio and hydrogen fraction. They found that a hydrogen volume fraction of about 10% can improve ignition and give the best efficiency and power. Frigo and Gentili et al. [83,84] modified a four-stroke twin-cylinder gasoline engine and supplied an ammonia–hydrogen mixture through the intake port. The detailed experimental setup is shown in Figure 9. Their results confirmed that hydrogen compensates for the low reactivity of ammonia and speeds up flame propagation. It also ensures stable combustion under different loads, although the overall performance remains lower than the original gasoline engine.

Additionally, Lhuillier et al. [85,86] tested ammonia/air, ammonia–hydrogen/air, and methane/air mixtures in a single-cylinder SI engine. They showed that near-stoichiometric ammonia can reach high combustion completeness. They also found that adding 20% hydrogen shortens the combustion duration, prevents misfire, and strongly enhances early heat release. Ji et al. [87] studied the effect of adding ammonia to a hydrogen engine under part load. Ammonia slowed the combustion rate and increased ignition delay, but it also raised the mean indicated pressure. Dinesh et al. [88] used a variable-compression-ratio engine to quantify hydrogen-assisted ammonia combustion. Higher compression ratios and higher hydrogen fractions increased the overall heat release rate and sped up early combustion (such as CA10). However, excessive hydrogen reduced volumetric efficiency and limited performance gains. Overall, adjusting the hydrogen ratio, equivalence ratio, compression ratio, and ignition strategy can effectively enhance ammonia reactivity. These studies support that hydrogen addition improves ignition stability and accelerates heat release.

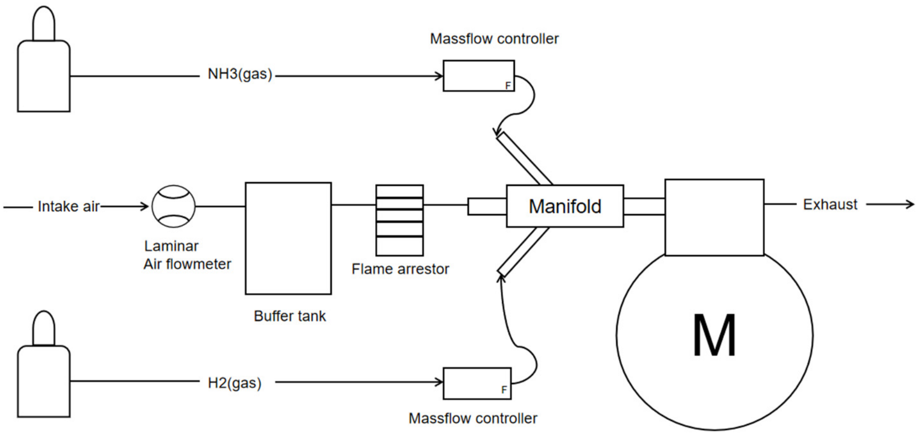

Figure 9. Schematic diagram of the ammonia–hydrogen fuel system configuration.

The emission studies mainly focus on the mechanisms and control challenges of NO_x (including thermal NO_x and fuel NO_x), ammonia (NH_3) slip, and N_2O formation during ammonia combustion. Ryu et al. [89] used gasoline intake ignition combined with liquid ammonia direct injection into the cylinder. They found that when ammonia was injected at 370° CA BTDC, the power was close to that of the gasoline mode, but NO_x emissions increased. This indicates that while direct injection improves charge quality, it also enhances high-temperature zones and fuel NO_x formation. Lhuillier et al. [85] compared ammonia/air and ammonia/hydrogen/air combustion under different equivalence ratios and intake pressures. They pointed out that a moderate amount of hydrogen can reduce fuel NO_x to some extent, while near-stoichiometric conditions result in lower NH_3 emissions and higher combustion completeness. Oh et al. [90] studied the emissions of a natural gas–ammonia dual-fuel turbocharged engine at full load (as shown in Figure 10). They found that when the ammonia energy fraction exceeded 5%, fuel NO_x dominated and increased monotonically with the ammonia ratio. Additionally, a lower excess air ratio led to a larger increase in NO_x.

Furthermore, Wei et al. [91] further studied marine natural gas engines and observed that, as X_{NH3} increased, NO_x emissions first increased and then decreased, while NH_3 and N_2O steadily increased. The primary source of NO_x was from the fuel pathway. Xin et al. [92,93] observed that adding ammonia to a hydrogen engine also resulted in an overall increase in NO_x emissions, and delaying ignition could not effectively suppress this increase. This suggests that, under hydrogen-enhanced combustion, the flame temperature remains high, making it difficult to control NO_x formation. Overall, existing research consistently highlights that the emission challenges in ammonia combustion are centered around fuel NO_x and NH_3 emissions, which are influenced by factors such as ammonia fraction, equivalence ratio, ignition timing, and hydrogen blending.

Studies on performance and efficiency mainly evaluate how ammonia, ammonia/hydrogen, and ammonia/natural gas blends affect output power, indicated thermal efficiency, and combustion losses under different operating conditions. Ryu et al. [83] studied the direct injection of ammonia. They showed that when gasoline provided the ignition energy and ammonia was injected early, the maximum output reached 2.7 kW. This was close to the gasoline mode. Their results indicate that a proper injection strategy can reduce the charge-loss problem caused by ammonia. Xin et al. [92,93] added a small amount of ammonia (about 2.2%) into a four-cylinder direct-injection hydrogen engine. They found that, under specific intake pressures and full-load conditions, both IMEP and indicated thermal efficiency increased. The main reason was that ammonia helped moderate the overly rapid heat release rate of hydrogen combustion, which improved the effective energy output. Oh et al. [90] tested a natural gas–ammonia dual-fuel engine. As the ammonia energy fraction increased, cooling losses decreased, but pumping losses and incomplete-combustion losses increased. As a result, the net indicated efficiency dropped slightly, but it still stayed near the natural gas baseline.

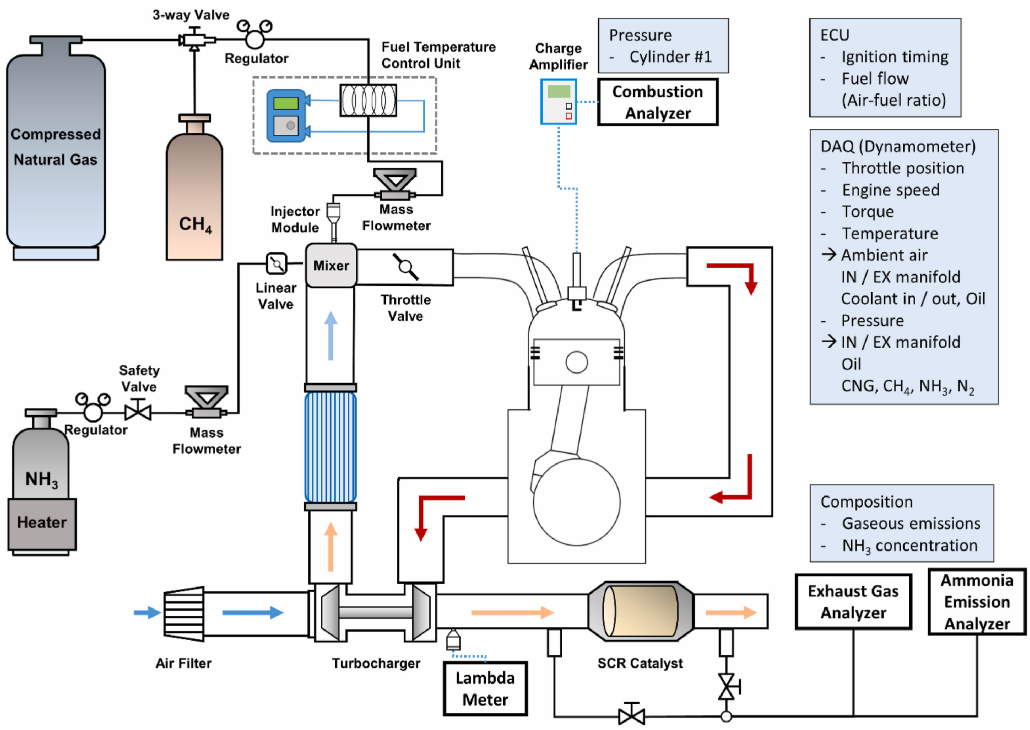

Figure 10. Experimental configuration of dual-fuel natural gas–ammonia spark ignition engine. Reproduced with permission from ref. [88]. Copyright 2021 Elsevier.

Moreover, Wei et al. [91] reported that, within a certain ammonia-blending range, thermal efficiency increased by about 1.96%. At the same time, CO_2 emissions decreased by up to 44%. These results show the potential benefit of replacing part of the natural gas with ammonia. Lhuillier et al. [85] also showed that near-stoichiometric operation allowed pure ammonia to reach a thermal efficiency comparable to methane. Dinesh et al. [88] found that increasing the compression ratio from 12 to 15 and raising the hydrogen energy share improved brake thermal efficiency by up to 33%. Overall, the studies show that optimizing ammonia fraction, intake pressure, hydrogen addition, ignition timing, and compression ratio can increase the effective heat release of ammonia combustion. With these strategies, engines can achieve efficiency levels close to or even higher than those of conventional gaseous fuels.

Table 3 shows the comparison of conventional spark ignition ammonia engines. Due to the high autoignition temperature and slow flame speed of ammonia, conventional SI ammonia engines rely on spark ignition. They usually require hydrogen, gasoline, or natural gas as assisting fuels. Existing studies consistently show that stable and efficient operation is difficult with pure ammonia. The addition of hydrogen or other reactive fuels can shorten the combustion duration, enhance early heat release, and improve cycle stability, as shown in Table 3. However, the overall performance is still generally lower than that of conventional gasoline engines.

Table 3. Comparative study on conventional spark ignition ammonia engines.

Authors	Fuel System	Measure	Conclusion
Mørch et al. [82]	NH_3/H_2/Air	Blend 10% hydrogen	The engine performs best in terms of efficiency and power.
Frigo and Gentili et al. [83,84]	NH_3/H_2/Air	The introduction of ammonia–hydrogen mixed gas	The introduction of hydrogen accelerates flame propagation.
Lhuillier et al. [85,86]	NH_3/H_2/Air	Adding 20% hydrogen	Shortens the combustion duration and increases the early heat release
Ji et al. [87]	H_2/NH_3/Air	Add ammonia to the hydrogen engine	Combustion rate decrease, ignition delay and IMEP
Xin et al. [93,94]	H_2/NH_3	Adding 2.2% ammonia to a hydrogen engine	IMEP and marked thermal efficiency are improved
Dinesh et al. [88]	NH_3/H_2	The influence of different hydrogen ratios on ammonia engines	The hydrogen ratio can increase the total heat release rate and accelerate the early combustion stage.
Wei et al. [91]	NG/NH_3	Ammonia mixed with natural gas	The thermal efficiency is increased by about 1.96%.

Overall, most studies focus on ignition behavior, flame propagation, cycle stability, and pollutant emissions (such as NO_x, ammonia slip, and N_2O). Moderate hydrogen blending, typically 10–20% by volume, can enhance ammonia reactivity and improve ignition reliability. Stable combustion can be achieved over a wide load range. Increasing the compression ratio and optimizing the equivalence ratio and ignition timing can further accelerate heat release and improve combustion efficiency. However, excessive hydrogen reduces volumetric efficiency, limits performance improvement and increases NO_x emissions. Future studies should focus on fuel blending optimization, ignition and intake strategy improvement, and effective after-treatment systems. It should also be noted that the commonly reported 10–20% hydrogen addition is mainly evaluated from the viewpoint of combustion improvement. In practical marine engines, the feasibility of this strategy depends on whether hydrogen is stored onboard, produced by ammonia cracking, or generated through exhaust-heat recovery, as each route has different implications for safety, volume, response time and system cost.

6.2. *Marine Pre-Chamber Jet Ignition Engine*

Ammonia-fueled engines with advanced ignition strategies demonstrate a more prominent advantage in greenhouse gas emission reduction. Specifically, ammonia-fueled engines adopting ammonia–hydrogen premixed pre-chamber jet ignition show great potential to overcome the existing power output limitations of ammonia-fueled power systems [94]. As a high-performance ignition technology, pre-chamber jet ignition is widely recognized as a key development direction for next-generation advanced ignition systems. For an ammonia-fueled engine configured with pre-chamber jet ignition, an independent pre-chamber is arranged, in which the high-reactivity mixture is ignited by a spark plug. After the ignition event, the in-pre-chamber combustion produces high-temperature and high-pressure gas jets, which are injected into the main combustion chamber through multiple small orifices. This process creates multiple distributed ignition sources in the main combustion chamber, enhancing both the ignition stability of the cylinder mixture and flame propagation velocity (as shown in Figure 11).

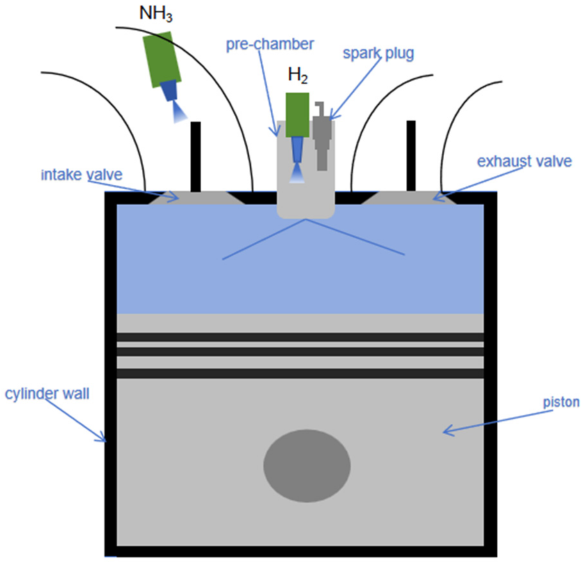

Figure 11. Working principle of PCJI ammonia-fueled engine.

The pre-combustion chamber can be divided into an active pre-combustion chamber and a passive pre-combustion chamber. The active pre-combustion chamber has additional fuel addition, while the passive pre-combustion chamber does not have it [95–97].

Zhao et al. [98] found that at a high compression ratio of 17:1, the jet flame tends to impact the combustion chamber walls, causing large-scale quenching. The heat release is rapid in the early combustion stage but slows down later, with unburned hydrocarbons in the clearance of the combustion chamber and pre-chamber aggravating afterburning and extending the combustion duration. Adding auxiliary fuel to the pre-chamber can increase the initial kinetic energy of the hot jet, improve the flame structure, and accelerate the consumption of the mixture in the main combustion chamber [99]. Zhou et al. [100] pointed out that pre-chamber jet ignition was superior to traditional spark plug ignition because it increased the ignition points in the main combustion chamber. The high-speed impact jets produced after ignition raised the turbulence intensity in the main combustion chamber, accelerating turbulent flame propagation. At 2000 rpm and 1.2 MPa indicated mean effective pressure, the 50% combustion angle in the pre-chamber engine was about 8.5° earlier than in the spark plug engine. With the increase in speed and load, this effect gradually decreases.

Liu et al. [101] designed an air-assisted pre-chamber to optimize spark ignition ammonia engine performance. Wang et al. [102] proposed a turbulent jet ignition strategy with auxiliary oxygen injection in the pre-chamber to improve the ignition and combustion performance of ammonia-rich/air mixtures. They found that injecting excess oxygen into the pre-chamber effectively enhanced ignition. The equivalence ratio of the pre-chamber had no significant effect on jet intensity, but increasing the equivalence ratio of the main combustion chamber and decreasing nozzle diameter increased jet velocity. However, ignition performance was affected by the competition between turbulence and mixture reactivity, requiring optimal turbulence intensity to promote rapid combustion. Table 4 shows the effect of pre-chamber jet ignition engine on combustion and emissions.

Table 4. The effect of pre-chamber jet ignition engine on combustion and emissions.

Authors	Key Technology	Operating Conditions	Combustion and Performance Indicators	Emission Characteristics
Zhao et al. [95]	Jet ignition	High compression ratio	Significantly prolonged combustion duration	Increased unburned HC due to enhanced afterburning
Sang et al. [96]	TJI with auxiliary fuel in pre-chamber	λ = 1.5	Maximum combustion pressure +66.4%	NO_x reduced by 93.9% compared with stoichiometric operation
Zhou et al. [97]	Passive pre-chamber jet ignition	2000 rpm, 1.2 MPa IMEP	CA50 advanced by ~8.5° CA	Not quantitatively reported
Liu et al. [98]	Air-assisted pre-chamber + TJI	Lean operation, λ = 1.4	Significant reduction in IMEP COV	NO_x and NH_3 emissions reduced
Wang et al. [99]	Oxygen-assisted pre-chamber TJI	Variable nozzle diameters	Jet velocity increases	Not quantitatively reported
Zhan et al. [100]	Active pre-chamber ignition	Different pre-chamber injection levels	Increased jet penetration	PM emissions increased with higher pre-chamber fuel supply
Liu et al. [101]	Air-assisted RCTJ pre-chamber + H_2	Intake temperature: 300 K	Shortest ignition delay and combustion duration for H_2–air mixture	Reduced NH_3 emissions (qualitative)

In emission performance research, Sang et al. [99] found that, at an excess air ratio of 1.5, NO_x emissions in the turbulent jet ignition mode were 93.9% lower than those in stoichiometric combustion. At the same time, Zhan et al. [103] pointed out that increasing the fuel injection in the active pre-chamber increased the penetration distance and wall impingement of the fuel jet, which led to higher particulate matter (PM) emissions. In addition, Liu et al. [104] developed a hydrogen-assisted ammonia combustion strategy within a pre-chamber. This approach was ultimately applied to an RCTJ pre-chamber to overcome combustion deficiencies and achieve efficient and stable combustion. The study also found that the use of different fuels can change the reactivity of the pre-combustion chamber mixture. The hydrogen–air mixture in the pre-combustion chamber has the shortest ignition delay time and combustion duration due to its highest reactivity.

In summary, the development of pre-chamber jet ignition (PCJI) technology and its application in ammonia-fueled engines enhance the ignition energy of the mixture in the main combustion chamber, achieve multi-point ignition, and accelerate flame propagation. Pre-chamber jet ignition technology provides a promising pathway for achieving high efficiency, low emissions, and stable combustion in ammonia-fueled engines. This technology not only effectively overcomes the ignition limitations of ammonia fuel but also offers crucial technical support and a viable direction for the future development of zero-carbon internal combustion engines.

To conclude the discussion of ammonia combustion modes in marine engines, a cross-comparison of the main emission characteristics is necessary because different engine concepts exhibit distinct NO_x and NH_3 slip behaviors. Table 5 summarizes the key differences among HCCI, PPC, HPDF, conventional SI, and pre-chamber jet ignition engines in terms of dominant combustion features, NO_x tendency, NH_3 slip tendency, and emission-control challenges.

Table 5. Key comparison of NO_x and NH_3 slip characteristics among representative ammonia combustion modes.

Combustion Mode	Dominant Combustion Feature	NO_x Tendency	NH_3 Slip Tendency	Key Emission-Control Challenge
HCCI	Premixed autoignition of NH_3/H_2 mixture	Increases with NH_3 fraction and combustion temperature; EGR can reduce NO_x but may lower efficiency	Mainly caused by incomplete oxidation and misfire-prone operation	Balancing ignition stability, combustion phasing, NO_x control, and unburned NH_3
PPC	Pilot-assisted or partially premixed NH_3/diesel combustion	May decrease at low NH_3 energy fraction, but increases at high NH_3 substitution due to fuel-bound nitrogen and incomplete combustion	Can be significant, especially under high NH_3 fraction or insufficient pilot ignition; split injection can reduce NH_3 slip	Simultaneous control of NO_x, NH_3 slip, CO/HC, and N_2O
HPDF	Diesel-pilot ignition with high-pressure NH_3 direct injection	Optimized spray–pilot interaction can reduce NO_x compared with low-pressure or premixed modes	Generally lower than intake-premixed modes, but increases if pilot energy or spray matching is insufficient	Maintaining high NH_3 substitution while avoiding unstable ignition and NH_3 slip
Conventional SI	Spark-ignited premixed NH_3/H_2, NH_3/gasoline, or NH_3/NG combustion	Fuel-bound NO_x often increases with NH_3 fraction; hydrogen addition may improve combustion but can raise NO_x	Reduced near stoichiometric and complete combustion conditions, but increases under poor flame propagation or quenching	Improving flame propagation while suppressing fuel-NO_x and residual NH_3
Pre-chamber jet ignition	Jet-assisted turbulent premixed deflagration	Lean operation and optimized jet ignition can reduce NO_x	Can be reduced by stronger ignition and faster flame propagation	Optimizing pre-chamber fueling, jet intensity, equivalence ratio, and NH_3/H_2 slip

Overall, the comparison shows that the emission issue of ammonia engines is not governed by a single pollutant, but by the coupled control of NO_x formation, unburned NH_3, combustion stability, and ammonia substitution ratio. HCCI engines are mainly limited by autoignition control and combustion phasing, while PPC engines require careful coordination of ammonia energy fraction, pilot-fuel timing, and injection strategy to avoid increased NO_x, NH_3 slip, CO/HC, and N_2O emissions. HPDF engines show stronger potential for marine applications because high-pressure ammonia injection can improve power density and reduce NH_3 slip, but their performance strongly depends on spray–pilot interaction and pilot-fuel quantity. For conventional SI engines, the major limitation is ammonia's slow flame propagation, which can lead to incomplete combustion and residual NH_3. In comparison, pre-chamber jet ignition enhances ignition energy and turbulent flame development, thereby offering a promising route to improve combustion stability while reducing NH_3 slip and controlling NO_x emissions under optimized lean-burn conditions.

7. Exhaust After-Treatment and NH_3 Slip Control

Although combustion optimization is essential for ammonia-fueled marine engines, in-cylinder control alone is unlikely to simultaneously eliminate NO_x, NH_3 slip, and N_2O

emissions under the variable operating conditions of practical marine propulsion systems. Across the combustion modes reviewed above, NO_x emissions are mainly associated with both thermal NO_x and fuel-bound NO_x pathways, while NH_3 slip originates from the incomplete oxidation of ammonia, local over-lean or over-rich mixtures, wall quenching, crevice effects, and insufficient residence time in low-temperature regions. In addition, N_2O may be formed during low-temperature ammonia oxidation and incomplete nitrogen conversion, which is particularly important because N_2O has a much higher global warming potential than CO_2. Therefore, exhaust after-treatment should not be considered as an optional auxiliary system, but as an indispensable part of ammonia engine development [105–107] (as shown in Figure 12).

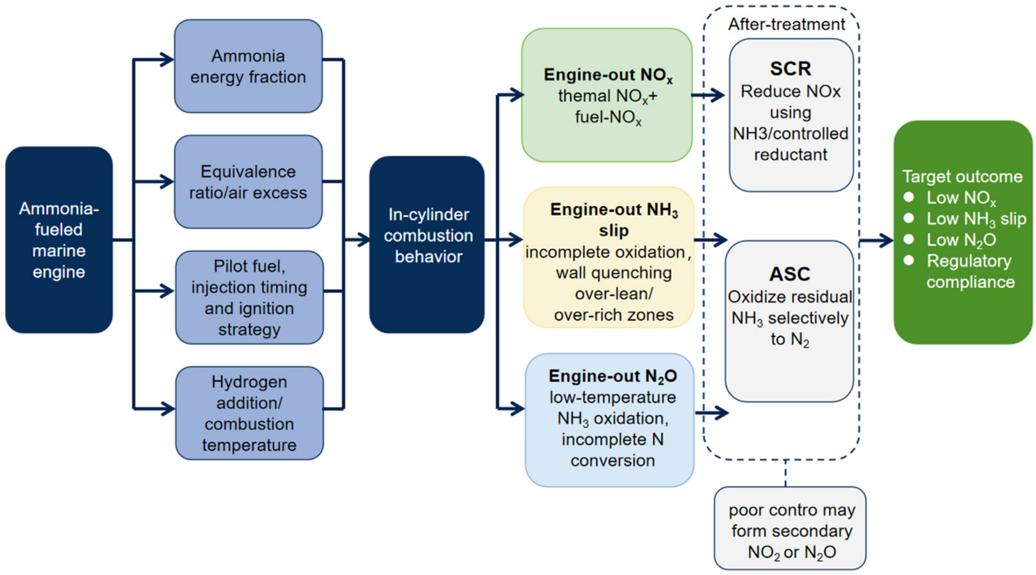

Figure 12. System-level control of NOx, NH_3 slip and N_2O.

Selective catalytic reduction (SCR) is particularly relevant for ammonia-fueled engines because NH_3 is already used as the reductant in conventional NO_x control systems. In typical SCR reactions, NH_3 reacts with NO and/or NO_2 over a catalyst surface to form N_2 and H_2O. The standard SCR reaction can be expressed as:

$$4NH_3 + 4NO + O_2 \rightarrow 4N_2 + 6H_2O$$

and the fast SCR reaction can be expressed as:

$$2NH_3 + NO + NO_2 \rightarrow 2N_2 + 3H_2O$$

For conventional diesel engines, the amount of injected urea or ammonia reductant can be actively controlled according to the measured NO_x concentration. However, in ammonia-fueled engines, the situation becomes more complex because NH_3 is both the fuel and a potential reductant. A certain amount of engine-out NH_3 may participate in NO_x reduction in the SCR catalyst, but uncontrolled NH_3 slip cannot be regarded as a harmless surplus reductant. It represents a toxic exhaust component, may cause odor and safety concerns, and can lead to secondary emissions if it is not properly converted downstream. Sun et al. coupled a three-dimensional ammonia–diesel dual-fuel engine model with a one-dimensional SCR model and showed that NO_x could be effectively reduced under many operating conditions, but excessive engine-out NH_3 could remain high after SCR when the NH_3 concentration in the exhaust was too large [108]. Therefore, the objective of the after-treatment system is not only high NO_x conversion efficiency, but also the simultaneous limitation of residual NH_3 and N_2O emissions.

Recent experimental studies further demonstrate this trade-off. Xiang et al. investigated an ammonia/diesel dual-fuel engine equipped with DOC + SCR after-treatment and reported that increasing the ammonia fraction increased NH_3, HC, CO and N_2O emissions, while NO_x emissions decreased. Although DOC could reduce NH_3 emissions by more than 90%, NH_3 oxidation in the DOC also produced NO_x and N_2O. The SCR system reduced NO_x, N_2O and NH_3 to some extent, but the N_2O conversion efficiency remained limited, and large amounts of NO_x and NH_3 could still appear at the SCR outlet under some conditions [105]. Similarly, Tyrewala et al. evaluated a commercial Cu–zeolite SCR and ammonia slip catalyst system on a high-load dual-fuel ammonia engine. Their results showed that SCR could achieve more than 99% NO_x conversion with less than 50 ppm NH_3 slip at air–fuel equivalence ratios greater than 1.4, but additional N_2O was formed over the Cu-SCR catalyst [106]. These findings indicate that SCR/ASC systems are promising for ammonia engines, but they must be optimized to avoid shifting the emission problem from NO_x and NH_3 to N_2O.

A practical after-treatment system for ammonia-fueled marine engines may therefore require a combined SCR and ammonia slip catalyst (ASC) configuration. In this layout, the SCR catalyst is responsible for reducing NO_x by using either controlled reductant dosing or engine-out NH_3, while the ASC is placed downstream to oxidize residual NH_3. Ideally, the ASC should selectively oxidize NH_3 to N_2 and H_2O:

$$4NH_3 + 3O_2 \rightarrow 2N_2 + 6H_2O$$

However, excessive or poorly controlled oxidation activity may generate undesirable NO_x or N_2O by-products, for example,

$$4NH_3 + 5O_2 \rightarrow 4NO + 6H_2O$$

$$2NH_3 + 2O_2 \rightarrow N_2O + 3H_2O$$

This trade-off makes catalyst selection and temperature control especially important. Ghosh et al. emphasized that ASC is an essential final step in the emission-control system because it selectively oxidizes NH_3 to N_2, and they proposed a Pt/Al_2O_3@Cu/ZSM-5 core–shell catalyst to improve low-temperature NH_3 conversion and N_2 selectivity [109]. Yao et al. developed a one-dimensional kinetic model for a dual-layer ASC consisting of Cu/SSZ-13 and Pt/Al_2O_3, showing that NH_3 conversion and N_2O selectivity are affected by the NO/NH_3 ratio and space velocity [110]. Therefore, the ASC should be evaluated not only by its NH_3 conversion efficiency, but also by its selectivity toward N_2 and its ability to suppress secondary N_2O formation.

Marine engines introduce additional challenges for SCR and ASC operation. Unlike stationary engines operating near steady-state conditions, marine propulsion engines often experience wide load variations, long low-load operation, acceleration and deceleration during maneuvering, and changes in exhaust temperature. At a low load, the exhaust temperature may be insufficient for high SCR activity, which can reduce NO_x conversion and increase NH_3 slip. At a high load, elevated exhaust temperature may improve catalytic activity but also increase thermal NO_x formation and promote undesired ammonia oxidation (as shown in Figure 13). In addition, marine fuels and lubricants may introduce sulfur-containing species, water vapor and particulate matter, which can affect catalyst durability and long-term activity. Brandenberger et al. summarized the complex reaction chemistry, undesired side reactions and catalyst mechanism issues of NH_3-SCR over metal-exchanged zeolites, while Jabłońska reviewed Cu-containing SSZ-13 catalysts for both NH_3-SCR-DeNO$_x$ and selective ammonia oxidation, including hydrothermal stability, poisoning resistance and reaction mechanisms [111,112]. These studies indicate that marine ammonia-engine after-treatment systems must be designed for a broad operating window rather than a single optimized point.

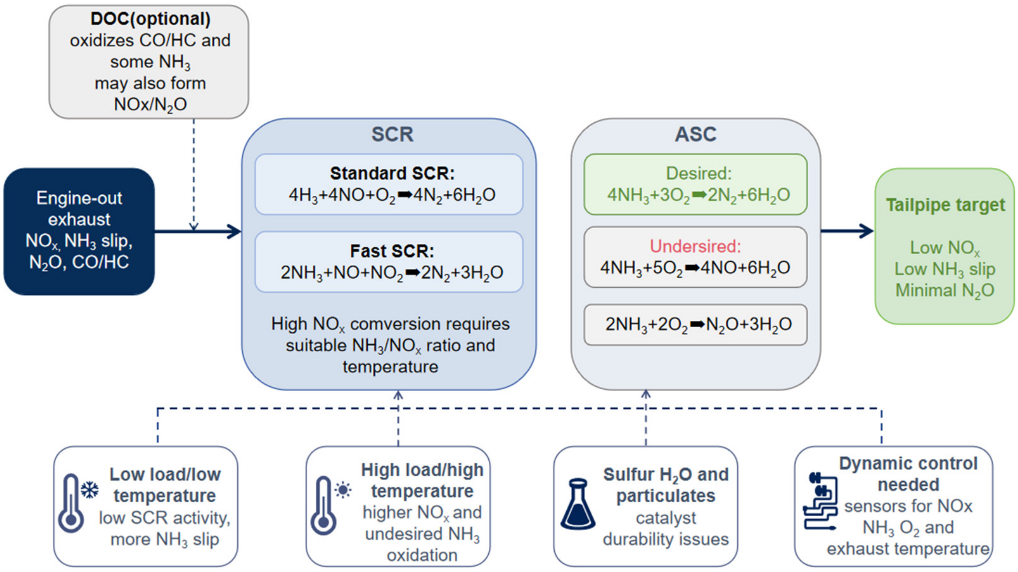

Figure 13. SCR–ASC after-treatment mechanism and operating trade-offs. (Solid arrows in figures denote actual exhaust flow and aftertreatment sequence; dashed arrows represent effects of operating conditions, control parameters or potential issues on aftertreatment units).

From a control perspective, the key parameter is the dynamic balance between engine-out NO_x and NH_3. If the NH_3/NO_x ratio is too low, NO_x conversion in the SCR catalyst is insufficient. If it is too high, residual NH_3 passes through the SCR catalyst and increases the burden on the downstream ASC. This problem is more difficult in ammonia engines than in conventional diesel engines because engine-out NH_3 slip is strongly affected by ammonia energy fraction, equivalence ratio, hydrogen addition, injection timing, ignition strategy and combustion completeness. Therefore, closed-loop control based on NO_x, NH_3, oxygen concentration and exhaust-temperature sensors may be necessary. Such a system should coordinate fuel injection, ignition timing, pilot-fuel quantity, hydrogen enrichment and SCR/ASC operation in real time.

Overall, NH_3 slip control should be treated as a system-level problem rather than a separate exhaust-cleaning issue. Increasing combustion temperature or hydrogen fraction may reduce unburned NH_3, but it can also increase NO_x formation. Operating at lean or low-temperature conditions may suppress NO_x, but it can increase NH3 slip and N_2O emissions. Similarly, SCR can reduce NO_x effectively, but inappropriate NH3 management may lead to excessive downstream NH_3 or secondary N_2O formation. Consequently, future ammonia-fueled marine engines should be developed through combustion–after-treatment co-optimization. For large marine engines, the most promising strategy is to combine stable in-cylinder ammonia combustion, minimized pilot-fuel consumption, controlled engine-out NH_3/NO_x ratio, efficient SCR conversion and highly selective ASC operation. This integrated approach is essential for achieving low NO_x, low NH_3 slip, low N_2O emissions and practical compliance with future marine emission regulations.

8. Conclusions

Research on ammonia-fueled marine engines has progressed from early feasibility verification to a clearer understanding of combustion-mode selection, fuel reactivity improvement, emission formation, and exhaust after-treatment. Current studies show that ammonia can be used in internal combustion engines, but its low chemical reactivity, high autoignition temperature, slow combustion rate, and nitrogen-containing molecular structure make stable combustion and emission control more difficult than for conventional hydrocarbon fuels. Different combustion concepts show different advantages and limitations. HCCI ammonia engines can achieve low-temperature and premixed autoignition combustion, but their operating range is narrow and strongly affected by ammonia fraction, hydrogen addition, intake temperature, compression ratio, and combustion phasing. PPC ammonia engines can extend the load range compared with HCCI and reduce CO_2 emissions through ammonia substitution, but NO_x, NH_3 slip, CO/HC, and N_2O emissions remain difficult to control. HPDF ammonia engines are more suitable for large marine engines because high-pressure ammonia direct injection can preserve intake-air charging efficiency, maintain power density, and achieve high ammonia substitution. However, their performance depends strongly on diesel pilot quantity, ammonia injection pressure, injector arrangement, and spray–pilot interaction. For spark ignition ammonia engines, hydrogen, gasoline, or natural gas blending can improve ignition and flame propagation, while pre-chamber jet ignition provides a promising route for enhancing lean combustion stability.

The reviewed studies also reveal several important contradictions. Increasing hydrogen addition, combustion temperature, or pilot-fuel quantity can improve combustion stability and reduce NH_3 slip, but it may also increase NO_x emissions, the pressure rise rate, system complexity, or residual fossil CO_2 emissions. Lean or low-temperature combustion can reduce thermal NO_x, but it may increase incomplete ammonia oxidation, NH_3 slip, and N_2O formation. Similarly, SCR and ASC systems can reduce NO_x and residual NH_3, but poorly controlled ammonia oxidation may generate secondary NO_x or N_2O. Therefore, ammonia-engine performance should not be evaluated only by CO_2 reduction or thermal efficiency. NO_x, NH_3 slip, N_2O, combustion stability, pilot-fuel consumption, and after-treatment selectivity must be considered together. The key bottleneck to commercialization is the lack of an integrated and durable combustion–after-treatment control system suitable for real marine operating conditions. In practical ammonia-fueled marine engines, NH_3 is simultaneously the fuel, a possible unburned toxic exhaust component, and a potential SCR reductant. This makes the dynamic balance between engine-out NH_3 and NO_x especially important. Future research should focus on large-bore marine-engine validation, HPDF ammonia injection and pilot ignition optimization, pre-chamber ignition development, onboard ammonia safety and corrosion control, ammonia cracking or hydrogen-supply strategies, and SCR/ASC systems with high NO_x conversion, high NH_3 conversion, low N_2O selectivity, and long-term durability. Only through coordinated optimization of combustion, fuel supply, control strategy, and after-treatment can ammonia-fueled marine engines become a practical route for deep decarbonization of shipping.

Author Contributions: Conceptualization, Y.C. and N.Z.; methodology, Y.C. and W.G.; validation, Y.C. and W.G.; investigation, Y.C. and N.Z.; resources, Y.C. and B.H.; data curation, Y.C.; writing—original draft preparation, Y.C.; writing—review and editing, Y.C., W.G. and B.H.; visualization, Y.C. and W.G.; supervision, B.H.; project administration, Y.C.; funding acquisition, Y.C. and N.Z. All authors have read and agreed to the published version of the manuscript.

Funding: This research was funded by the National Natural Science Foundation of China (no. 52301382), Nature Science Foundation of Hubei Province (no. 52301382), Key Laboratory of Automotive Power Train and Electronics Control (Hubei University of Automotive Technology) (no. ZDK12024B10), and Nature Science Foundation of Hubei Province (no. 2025AFD230), and a start-up fund for doctoral research (Hubei University of Automotive Technology) (no. BK202427).

Data Availability Statement: No new data were created or analyzed in this study. Data sharing is not applicable to this article.

Conflicts of Interest: The authors declare no conflicts of interest.

Abbreviations

Abbreviation	Full term	Description
GHG	Greenhouse Gas	Gaseous compounds that trap heat in the atmosphere, such as CO_2, CH_4, N_2O, and others.
CO_2	Carbon Dioxide	The primary greenhouse gas emitted through human activities.
CH_4	Methane	A potent greenhouse gas with high global warming potential.
N_2O	Nitrous Oxide	A greenhouse gas mainly produced by agricultural and combustion processes.
HCCI	Homogeneous Charge Compression Ignition	A combustion mode that simultaneously ignites a premixed fuel–air mixture via compression.
PPC	Partially Premixed Combustion	A combustion mode that blends characteristics of diesel and gasoline combustion for high efficiency.
HPDF	High Pressure Dual Fuel	Combustion system using dual injection (typically diesel + ammonia or hydrogen) under high pressure.
SI	Spark Ignition	Conventional ignition using spark plugs, similar to gasoline engines.
TJI	Turbulent Jet Ignition	An advanced ignition system using pre-chamber hot jets to enhance combustion rate.
EGR	Exhaust Gas Recirculation	A method to reduce NO_x emissions by recirculating a portion of exhaust gas into the intake.
NO_x	Nitrogen Oxides	Harmful nitrogen compounds produced during combustion, including NO and NO_2.
IMEP	Indicated Mean Effective Pressure	A measure of engine power output per cycle, reflecting combustion efficiency.
CA10–CA90	Crank Angle 10–90%	The crank angle interval over which 10–90% of the fuel mass is burned.
λ (Lambda)	Excess Air Ratio	The ratio of actual air/fuel ratio to the stoichiometric air/fuel ratio; indicates lean or rich combustion.
RON	Research Octane Number	A measure of a fuel's resistance to knock under standard test conditions.
LTC	Low-Temperature Combustion	Combustion strategy aimed at reducing NO_x and soot emissions.
NH_3	Ammonia	Zero-carbon fuel under study for internal combustion engines and marine propulsion.
H_2	Hydrogen	A clean, high-reactivity fuel often blended with ammonia to improve ignition and combustion.
DME	Dimethyl Ether	Alternative fuel used as ignition promoter in ammonia dual-fuel systems.
EEDI	Energy Efficiency Design Index	IMO metric to measure energy efficiency of ships.
IMO	International Maritime Organization	UN agency responsible for regulating shipping emissions and efficiency.

References

1. IPCC. Available online: https://www.ipcc.ch/report/ar6/wg1/ (accessed on 9 November 2025).
2. IPCC. Available online: https://www.ipcc.ch/report/ar6/wg1/downloads/faqs/IPCC_AR6_WGI_FAQs_Compiled.pdf (accessed on 9 November 2025).
3. Fischer, E.M.; Sippel, S.; Knutti, R. Increasing probability of record-shattering climate extremes. *Nat. Clim. Change* **2021**, *11*, 689–695. [CrossRef]
4. Friedlingstein, P.; O'sullivan, M.; Jones, M.W.; Andrew, R.M.; Hauck, J.; Olsen, A.; Peters, G.P.; Peters, W.; Pongratz, J.; Sitch, S.; et al. Global carbon budget 2020. *Earth Syst. Sci. Data* **2020**, *12*, 3269–3340. [CrossRef]

5. Etminan, M.; Myhre, G.; Highwood, E.J.; Shine, K.P. Radiative forcing of carbon dioxide, methane, and nitrous oxide: A significant revision of the methane radiative forcing. *Geophys. Res. Lett.* **2016**, *43*, 12614–12623. [CrossRef]
6. Velders, G.J.M.; Fahey, D.W.; Daniel, J.S.; McFarland, M.; Andersen, S.O. The large contribution of projected HFC emissions to future climate forcing. *Proc. Natl. Acad. Sci. USA* **2009**, *106*, 10949–10954. [CrossRef] [PubMed]
7. Skeie, R.B.; Hodnebrog, Ø.; Myhre, G. Trends in atmospheric methane concentrations since 1990 were driven and modified by anthropogenic emissions. *Commun. Earth Environ.* **2023**, *4*, 317. [CrossRef]
8. Makarova, M.; Poberovskii, A.; Polyakov, A.; Imkhasin, K.H.; Ionov, D.; Makarov, B.; Kostsov, V.; Foka, S.; Abakumov, E. Trends of key greenhouse gases as measured in 2009–2022 at the FTIR station of St. Petersburg State University. *Remote Sens.* **2024**, *16*, 1996. [CrossRef]
9. Sazu, A.V.F. Assessing The Effects of GDP and FDI Inflows on Carbon Dioxide Emission. *J. Dev. Econ. Soc. Stud.* **2025**, *4*, 289–302. [CrossRef]
10. NOAA. Available online: https://gml.noaa.gov/aggi/ (accessed on 9 November 2025).
11. Mao, X.; Meng, Z.; Comer, B.; Decker, T. *Greenhouse Gas Emissions and Air Pollution from Global Shipping, 2016–2023*; International Council on Clean Transportation: Washington, DC, USA, 2025; pp. 1–24. Available online: https://theicct.org/publication/greenhouse-gas-emissions-and-air-pollution-from-global-shipping-2016-2023-apr25/ (accessed on 9 November 2025).
12. Shuai, S.J.; Wang, Z.; Ma, X.; Xu, H.; He, X.; Wang, J. Low-carbon and zero-carbon technology paths and key technologies of internal combustion engines under the background of carbon neutrality. *J. Automot. Saf. Energy* **2021**, *12*, 417–439. [CrossRef]
13. Yuvenda, D.; Sudarmanta, B.; Wahjudi, A.; Muraza, O. Improved combustion performance and lowered emissions of CNG-diesel dual fuel engine under low load by optimizing CNG injection parameters. *Fuel* **2020**, *269*, 117202. [CrossRef]
14. Wang, H.Y.; Lu, C.H.; Wang, S.; Dong, Q. Influence of combustion chamber shape on the combustion characteristics of marine natural gas engine. *J. Harbin Eng. Univ.* **2022**, *43*, 1133–1138.
15. Serra, P.; Fancello, G. Towards the IMO's GHG Goals: A Critical Overview of the Perspectives and Challenges of the Main Options for Decarbonizing International Shipping. *Sustainability* **2020**, *12*, 3220. [CrossRef]
16. Dierick, J.; Sikleghem, L.; Verhelst, S. Efficiency and Emissions of a High-speed Marine Diesel Engine Converted to Dual-fuel Operation with Methanol. *Fuel* **2019**, *254*, 115662.
17. Ning, D.Z.; Guan, W.; Yang, K.; Wang, P.; Sheng, L.; Gao, Q. Influence of combustion chamber structures on engine in-cylinder gas flow in a methanol-fuelled heavy-duty engine. *Intern. Combust. Engine Powerpl.* **2022**, *39*, 14–21. [CrossRef]
18. Prante, G.A.F.; Santos, N.D.S.A.; Martins, M.E.S. Feasibility of replacing diesel with ethanol blended with biodiesel and diethyl-ether blends in a compression ignition engine. *J. Braz. Soc. Mech. Sci. Eng.* **2023**, *45*, 60. [CrossRef]
19. Khan, M.M.; Kadian, A.K.; Sharma, R.P. Attempt to mitigate marine engine emissions with improved performance by the investigation of alcohol inclusion in sunflower biodiesel-sunflower oil-diesel blend. *Environ. Sci. Pollut. Res. Int.* **2023**, *30*, 33974–33991. [PubMed]
20. Liu, Z.Q. *Joint Development of Ammonia-Fueled LNG Carriers by Mitsui O.S.K. Lines, Tsuneishi Shipbuilding, and Mitsui E&S Holdings*; Tsuneishi Shipbuilding: Fukuyama, Japan, 2022.
21. Martins, J.; Brito, F.P. Alternative fuels for international combustion engines. *Energies* **2020**, *13*, 4086. [CrossRef]
22. Cao, J.W.; Qin, X.F.; Geng, G.; Zhang, W.; Yu, B. Current status and prospects of hydrogen storage and transportation technology. *Acta Pet. Sin.* **2021**, *37*, 1461–1478. [CrossRef]
23. Gao, J.L.; Yuan, Z.M.; Shang, H.W.; Yong, H.; Qi, Y. Research progress on storage technology and stored energy application of hydrogen. *Metall. Funct. Mater.* **2016**, *23*, 1–11. [CrossRef]
24. Guo, P.Y.; Liu, Z.C.; Shao, F.G.; Shen, F.; Chen, L. Analysis of the application of hydrogen/ammonia fuel in the engine. *Autom. Pract. Technol.* **2016**, *4*, 81–84.
25. Li, J.B.; Wang, M.H. Economic analysis of ammonia mixed coal-fired power generation technology based on different scenario modes. *China Coal* **2022**, *48*, 54–59.
26. Chen, B.Q.; Liu, E.S. Review of the development of South Korea's shipbuilding industry in 2021. *China Ship Surv.* **2022**, *2*, 52–58.
27. DNV. Available online: https://www.dnv.com/energy-transition-outlook/carbon-capture-storage/ (accessed on 20 October 2025).
28. Ammonia Energy Association. Available online: https://ammoniaenergy.org/articles/renewable-ammonia-in-china-full-speed-ahead (accessed on 9 November 2025).
29. The Net-Zero Industry Tracker. Available online: https://www.weforumasia.cn/publications/the-net-zero-industry-tracker/in-full/ammonia-industry/ (accessed on 9 November 2025).
30. RMI. Available online: https://rmi.org.cn/wp-content/uploads/2024/11/0110%E7%BB%BF%E6%B0%A8%E6%8A%A5%E5%91%8A_%E6%89%A7%E8%A1%8C%E6%91%98%E8%A6%81.pdf (accessed on 4 July 2026).
31. Reuters. Available online: https://www.marinelink.com/news/zerocarbon-ammonia-shipping-faces-cost-518638 (accessed on 9 November 2025).
32. Nayak-Luke, R.M.; Bañares-Alcántara, R. Techno-economic viability of islanded green ammonia as a carbon-free energy vector and as a substitute for conventional production. *Energy Environ. Sci.* **2020**, *13*, 2957–2966. [CrossRef]

33. Li, J.; Lai, S.; Chen, D.; Wu, R.; Kobayashi, N.; Deng, L.; Huang, H. A review on combustion characteristics of ammonia as a carbon-free fuel. *Front. Energy Res.* **2021**, *9*, 760356. [CrossRef]
34. Shafie, P.; DeChamplain, A.; Lepine, J. Technical, environmental and economic analysis of utilizing hydrogen-rich fuel in decarbonized container ships. *Sustain. Energy Fuels* **2025**, *9*, 185–197. [CrossRef]
35. Tornatore, C.; Marchitto, L.; Sabia, P.; De Joannon, M. Ammonia as green fuel in internal combustion engines: State-of-the-art and future perspectives. *Front. Mech. Eng.* **2022**, *8*, 944201. [CrossRef]
36. Wu, H.; Mi, S.; Qian, Y.; Zhang, T.; Zhang, J.; Pan, C.; Shi, L.; Lu, X. Spray and evaporation characteristics of high-pressure liquid ammonia injection under flash-boiling and evaporating conditions. *Fuel* **2025**, *381*, 133627. [CrossRef]
37. Werrell, K.P. The Strategic Bombing of Germany in World War II: Costs and Accomplishments. *J. Am. Hist.* **1986**, *73*, 702–713. [CrossRef]
38. Koch, E. Ammonia–A fuel for motor buses. *J. Inst. Pet.* **1945**, *31*, 213.
39. Cornelius, W.; Huellmantel, L.W.; Mitchell, H.R. Ammonia as an engine fuel. *SAE Trans.* **1966**, *74*, 300–326. [CrossRef] [PubMed]
40. Starkman, E.S.; Newhall, H.K.; Sutton, R.; Maguire, T.; Farbar, L. Ammonia as a spark ignition engine fuel: Theory and application. *SAE Trans.* **1967**, *75*, 765–784. [CrossRef]
41. Gray, J.T., Jr.; Dimitroff, E.; Meckel, N.T.; Quillian, R.D. Ammonia fuel—Engine compatibility and combustion. *SAE Trans.* **1967**, *75*, 785–807. [CrossRef] [PubMed]
42. Pearsall, T.J.; Garabedian, C.G. Combustion of anhydrous ammonia in diesel engines. *SAE Trans.* **1968**, *76*, 3213–3221. [CrossRef] [PubMed]
43. Bro, K.; Pedersen, P. *Alternative Diesel Engine Fuels: An Experimental Investigation of Methanol, Ethanol, Methane and Ammonia in a D.I. Diesel Engine with Pilot Injection*; SAE Technical Paper 1977, 770794; SAE International: Warrendale, PA, USA, 1977. [CrossRef] [PubMed]
44. Yao, M.F.; Liu, H.F. Review and of the combustion technology of homogeneous charge compression lgnition and low temperature combustion. *Chin. J. Automot. Eng.* **2012**, *2*, 79–90. [CrossRef]
45. Yao, C.D.; Jing, Z.C.; Fu, X.G.; Liu, W.S.; Fu, D.C. Effects of cooled EGR on NOx emission and performances of gasoline engine. *Automot. Eng.* **2003**, *25*, 537–540.
46. Pochet, M.; Truedsson, I.; Foucher, F.; Jeanmart, H.; Contino, F. *Ammonia-Hydrogen Blends in Homogeneous-Charge Compression-Ignition Engine*; SAE Technical Paper 2017-24-0087; SAE International: Warrendale, PA, USA, 2017. [CrossRef]
47. Pochet, M.; Jeanmart, H.; Contino, F. A 22: 1 compression ratio ammonia-hydrogen HCCI engine: Combustion, load, and emission performances. *Front. Mech. Eng.* **2020**, *6*, 43. [CrossRef]
48. Wang, C.; Deng, J.; Ding, W.; Huang, Y.; Tang, Y.; Li, L. Thermodynamic analysis of employing argon as the diluent and adding hydrogen in an HCCI ammonia engine: Ignition characteristics and performances of combustion and NO emissions. *Int. J. Hydrogen Energy* **2024**, *49*, 293–300. [CrossRef]
49. Yan, Y.; Liu, Z.; Liu, J. Computational analysis of ammonia-hydrogen blends in homogeneous charge compression ignition engine operation. *Process Saf. Environ. Prot.* **2024**, *190*, 1263–1272. [CrossRef]
50. Balogun, F.; Vasudev, A.; Kakoee, A.; Sirviö, K.; Mikulski, M. Simulation-Based Study of NH_3/H_2-Dual Fueled HCCI Engine Performance: Effects of Blending Ratio, Equivalence Ratio, and Compression Ratio Using Detailed Chemical Kinetic Modeling. *J. Dev. Econ. Soc. Stud.* **2025**, *12*, 2049. [CrossRef]
51. Zhao, F.; Asmus, T.W.; Assanis, D.N.; Dec, J.E.; Eng, J.A.; Najt, P.M. (Eds.) *Homogeneous Charge Compression Ignition (HCCI) Engines—Key Research and Development Issues*; Society of Automotive Engineers: Warrendale, PA, USA, 2003; Volume 94, pp. 241–250.
52. Yao, M.; Zheng, Z.; Liu, H. Progress and recent trends in homogeneous charge compression ignition (HCCI) engines. *Prog. Energy Combust. Sci.* **2009**, *35*, 398–437. [CrossRef]
53. Manente, V.; Johansson, B.; Cannella, W. Gasoline partially premixed combustion, the future of internal combustion engines? *Int. J. Eng. Res.* **2011**, *12*, 194–208. [CrossRef]
54. Noehre, C.; Andersson, M.; Johansson, B.; Hultqvist, A. *Characterization of Partially Premixed Combustion*; SAE technical paper 2006-01-3412; SAE International: Warrendale, PA, USA, 2006. [CrossRef]
55. Reiter, A.J.; Kong, S.C. Combustion and emissions characteristics of compression-ignition engine using dual ammonia-diesel fuel. *Fuel* **2011**, *90*, 87–97. [CrossRef]
56. Reiter, A.J.; Kong, S.C. Demonstration of compression-ignition engine combustion using ammonia in reducing greenhouse gas emissions. *Energy Fuels* **2008**, *22*, 2963–2971. [CrossRef]
57. Gill, S.S.; Chatha, G.S.; Tsolakis, A.; Golunski, S.E.; York, A.P.E. Assessing the effects of partially decarbonising a diesel engine by co-fuelling with dissociated ammonia. *Int. J. Hydrogen Energy* **2012**, *37*, 6074–6083. [CrossRef]
58. Gross, C.W.; Kong, S.C. Performance characteristics of a compression-ignition engine using direct-injection ammonia–DME mixtures. *Fuel* **2013**, *103*, 1069–1079. [CrossRef]

59. Niki, Y.; Yoo, D.H.; Hirata, K.; Sekiguchi, H. Effects of ammonia gas mixed into intake air on combustion and emissions characteristics in diesel engin. In Proceedings of the ASME 2016 Internal Combustion Engine Division Fall Technical Conference, Greenville, SC, USA, 9–12 October 2016. [CrossRef]
60. Niki, Y.; Nitta, Y.; Sekiguchi, H.; Hirata, K. Diesel fuel multiple injection effects on emission characteristics of diesel engine mixed ammonia gas into intake air. *J. Eng. Gas Turbines Power* **2019**, *141*, 061020. [CrossRef]
61. Yousefi, A.; Guo, H.; Dev, S.; Liko, B.; Lafrance, S. Effects of ammonia energy fraction and diesel injection timing on combustion and emissions of an ammonia/diesel dual-fuel engine. *Fuel* **2022**, *314*, 122723. [CrossRef]
62. Yousefi, A.; Guo, H.; Dev, S.; Lafrance, S.; Liko, B. A study on split diesel injection on thermal efficiency and emissions of an ammonia/diesel dual-fuel engine. *Fuel* **2022**, *316*, 123412. [CrossRef]
63. Nadimi, E.; Przybyła, G.; Emberson, D.; Løvås, T.; Ziółkowski, Ł.; Adamczyk, W. Effects of using ammonia as a primary fuel on engine performance and emissions in an ammonia/biodiesel dual-fuel CI engine. *Int. J. Energy Res.* **2022**, *46*, 15347–15361. [CrossRef]
64. Niki, Y. Reductions in unburned ammonia and nitrous oxide emissions from an ammonia-assisted diesel engine with early timing diesel pilot injection. *J. Eng. Gas Turbines Power* **2021**, *143*, 091014. [CrossRef]
65. Lasocki, J.; Bednarski, M.; Sikora, M. Simulation of ammonia combustion in dual-fuel compression-ignition engine. *IOP Conf. Ser. Earth Environ. Sci.* **2019**, *214*, 012081. [CrossRef]
66. Kane, S.P.; Zarling, D.; Northrop, W.F. Thermochemical and sensible energy recuperation using thermally-integrated reactor and diesel-ammonia dual fueling strategy. In Proceedings of the ASME 2019 Internal Combustion Engine Division Fall Technical Conference, Chicago, IL, USA, 20–23 October 2019. [CrossRef]
67. Kane, S.P.; Northrop, W.F. Thermochemical recuperation to enable efficient ammonia-diesel dual-fuel combustion in a compression ignition engine. *Energies* **2021**, *14*, 7540. [CrossRef]
68. Liu, L.; Wu, Y.; Wang, Y. Numerical investigation on the combustion and emission characteristics of ammonia in a low-speed two-stroke marine engine. *Fuel* **2022**, *314*, 122727. [CrossRef]
69. Frankl, S.; Gleis, S. Development of a 3D-computational fluid dynamics model for a full optical high-pressure dual-fuel engine. *SAE Int. J. Engines* **2020**, *13*, 241–252. [CrossRef]
70. Dong, Y.; Kaario, O.; Hassan, G.; Ranta, O.; Larmi, M.; Johansson, B. High-pressure direct injection of methanol and pilot diesel: A non-premixed dual-fuel engine concept. *Fuel* **2020**, *277*, 117932. [CrossRef]
71. Liu, H.; Li, J.; Wang, J.; Wu, C.; Liu, B.; Dong, J.; Liu, T.; Ye, Y.; Wang, H.; Yao, M. Effects of injection strategies on low-speed marine engines using the dual fuel of high-pressure direct-injection natural gas and diesel. *Energy Sci. Eng.* **2019**, *7*, 1994–2010. [CrossRef]
72. Gleis, S.; Frankl, S.; Waligorski, D.; Prager, D.-I.M.; Wachtmeister, G. Investigation of the High-Pressure-Dual-Fuel (HPDF) combustion process of natural gas on a fully optically accessible research engine. *SAE Rep.* **2019**, *12*, 15. [CrossRef]
73. Frankl, S.; Gleis, S.; Karmann, S.; Prager, M.; Wachtmeister, G. Investigation of ammonia and hydrogen as CO_2-free fuels for heavy duty engines using a high pressure dual fuel combustion process. *Int. J. Engine Res.* **2021**, *22*, 3196–3208. [CrossRef]
74. Frankl, S.G.; Gelner, A.D.; Gleis, S.; Härtl, M.; Wachtmeister, G. Numerical study on renewable and sustainable fuels for HPDF engine. In Proceedings of the ASME Power Conference, Anaheim, CA, USA, 4–5 August 2020. [CrossRef]
75. Li, T.; Zhou, X.; Wang, N.; Wang, X.; Chen, R.; Li, S.; Yi, P. A comparison between low-and high-pressure injection dual-fuel modes of diesel-pilot-ignition ammonia combustion engines. *J. Energy Inst.* **2022**, *102*, 362–373. [CrossRef]
76. Sun, X.; Jiang, Y.C.; Zhao, P.; Jing, G.; Ma, T. Effect of ammonia/hydrogen blending and injection modes on combustion emission and performance of marine engine. *Fuel* **2024**, *371*, 131894. [CrossRef]
77. Wang, B.; Wang, H.; Duan, B.; Yang, C.; Hu, D.; Wang, Y. Effect of ammonia/hydrogen mixture ratio on engine combustion and emission performance at different inlet temperatures. *Energy* **2023**, *272*, 127110. [CrossRef]
78. Scharl, V.; Sattelmayer, T. Ignition and combustion characteristics of diesel piloted ammonia injections. *Fuel Commun.* **2022**, *11*, 100068. [CrossRef]
79. Zhou, X.; Li, T.; Wang, N.; Wang, X.; Chen, R.; Li, S. Pilot diesel-ignited ammonia dual fuel low-speed marine engines: A comparative analysis of ammonia premixed and high-pressure spray combustion modes with CFD simulation. *Renew. Sustain. Energy Rev.* **2023**, *173*, 113108. [CrossRef]
80. Zhang, Z.; Long, W.; Dong, P.; Tian, H.; Tian, J.; Li, B.; Wang, Y. Performance characteristics of a two-stroke low speed engine applying ammonia/diesel dual direct injection strategy. *Fuel* **2023**, *332*, 126086. [CrossRef]
81. Ambalakatte, A.; Geng, S.; Cairns, A.; Harrington, A.; Hall, J.; Bassett, M. Evaluation of ammonia-gasoline co-combustion in a modern spark ignition research engine. *Carbon Neutrality* **2023**, *2*, 35. [CrossRef]
82. Mørch, C.S.; Bjerre, A.; Gøttrup, M.P.; Sorenson, S.; Schramm, J. Ammonia/hydrogen mixtures in an SI-engine: Engine performance and analysis of a proposed fuel system. *Fuel* **2011**, *90*, 854–864. [CrossRef]
83. Frigo, S.; Gentili, R. Analysis of the behaviour of a 4-stroke Si engine fuelled with ammonia and hydrogen. *Int. J. Hydrogen Energy* **2013**, *38*, 1607–1615. [CrossRef]

84. Frigo, S.; Gentili, R.; Ricci, G.; Pozzana, G.; Comotti, M. Experimental results using ammonia plus hydrogen in a SI engine. In Proceedings of the FISITA 2012 World Automotive Congress, Beijing, China, 27–30 November 2012. [CrossRef]
85. Lhuillier, C.; Brequign, P.; Contino, F.; Rousselle, C. Combustion characteristics of ammonia in a modern spark-ignition engine. In *Proceedings of the Conference on Sustainable Mobility, Catania, Italy, 14 November 2019*; SAE International: Warrendale, PA, USA, 2019. [CrossRef]
86. Lhuillier, C.; Brequigny, P.; Contino, F.; Mounaïm-Rousselle, C. Experimental study on ammonia/hydrogen/air combustion in spark ignition engine conditions. *Fuel* **2020**, *269*, 117448. [CrossRef]
87. Ji, C.; Xin, G.; Wang, S.; Cong, X.; Meng, H.; Chang, K.; Yang, J. Effect of ammonia addition on combustion and emissions performance of a hydrogen engine at part load and stoichiometric conditions. *Int. J. Hydrogen Energy* **2021**, *46*, 40143–40153. [CrossRef]
88. Dinesh, M.H.; Pandey, J.K.; Kumar, G.N. Study of performance, combustion, and NOx emission behavior of an SI engine fuelled with ammonia/hydrogen blends at various compression ratio. *Int. J. Hydrogen Energy* **2022**, *47*, 25391–25403. [CrossRef]
89. Ryu, K.; Zacharakis-Jutz, G.E.; Kong, S.C. Effects of gaseous ammonia direct injection on performance characteristics of a spark-ignition engine. *Appl. Energy* **2014**, *116*, 206–215. [CrossRef]
90. Oh, S.; Park, C.; Oh, J.; Kim, S.; Kim, Y.; Choi, Y.; Kim, C. Combustion, emissions, and performance of natural gas–ammonia dual-fuel spark-ignited engine at full-load condition. *Energy* **2022**, *258*, 124837.
91. Wei, W.; Li, G.; Zhang, Z.; Long, Y.; Zhang, H.; Huang, Y.; Zhou, M.; Wei, Y. Effects of ammonia addition on the performance and emissions for a spark-ignition marine natural gas engine. *Energy* **2023**, *272*, 127092. [CrossRef]
92. Xin, G.; Ji, C.; Wang, S.; Meng, H.; Chang, K.; Yang, J. Effect of ammonia addition on combustion and emission characteristics of hydrogen-fueled engine under lean-burn condition. *Int. J. Hydrogen Energy* **2022**, *47*, 9762–9774.
93. Xin, G.; Ji, C.; Wang, S.; Meng, H.; Chang, K.; Yang, J. Effect of different volume fractions of ammonia on the combustion and emission characteristics of the hydrogen-fueled engine. *Int. J. Hydrogen Energy* **2022**, *47*, 16297–16308. [CrossRef]
94. Bychkov, V.; Valiev, D.; Eriksson, L.E. Physical mechanism of ultrafast flame acceleration. *Phys. Rev. Lett.* **2008**, *101*, 164501. [CrossRef] [PubMed]
95. Wang, B.Y.; Qi, Y.L.; Wang, Y.D.; Wang, Z.; Wang, J.X. An Investigation into the design and performance of Pre-combusition chamber jet igniter. *Automot. Eng.* **2018**, *40*, 7–13.
96. Li, X.; Feng, M.Z.; Zheng, S.B.; Huang, L.; Huang, Z. An Experimental Research of Lean-Burn Combustion Characteristics on a Pre-Chamber Marine Natural Gas Engine. *J. Intern. Combust. Engines* **2023**, *41*, 324–331.
97. Ye, Y.; Dong, J.J.; Wang, H.; Liu, T.; Liu, H.F.; Yao, M.F. Numerical simulation of the effect of Pre-chamber flame jet to combustion process on diesel-ng dual fuel engine. *CICEE* **2018**, *39*, 22–28. [CrossRef]
98. Zhao, Z.Q.; Cai, K.Y.; Wang, Z. Combustion and emission characteristics of high compression ratio jet ignition natural gas engine. *TICE* **2022**, *40*, 10–19. [CrossRef]
99. Sang, H.L.; Jiang, S.J.; Li, Z.J. Simulation on combustion characteristic of turbulent jet ignition. *Veh. Eng.* **2022**, *0*, 12–18. [CrossRef]
100. Zhou, H.; Han, Z.Y.; Wu, Z.K.; Meng, S. Numerical analysis of the stoichiometric-combustion characteristic of a gasoline engine with a passive pre-chamber. *CICEE* **2022**, *43*, 18–26. [CrossRef]
101. Liu, Z.; Zhou, L.; Zhong, L.; Wei, H. Enhanced combustion of ammonia engine based on novel air-assisted pre-chamber turbulent jet ignition. *Energy Convers. Manag.* **2023**, *276*, 116526. [CrossRef]
102. Wang, Z.; Ji, C.; Wang, D.; Zhang, T.; Wang, S.; Yang, H.; Zhai, Y.; Wang, H. Experimental investigation on combustion characteristics of ammonia/air using turbulent jet ignition with auxiliary oxygen in pre-chamber. *Appl. Therm. Eng.* **2024**, *243*, 122622. [CrossRef]
103. Zhan, W.F.; Luo, H.B.; Chen, H.; Li, Y.H.; Du, J. Effect of pre-chamber jet ignition on gasoline engine performance. *TICE* **2022**, *40*, 193–199. [CrossRef]
104. Liu, Z.; Zhou, L.; Zhong, L.; Wei, H. Reactivity controlled turbulent jet ignition (RCTJI) for ammonia engine. *Int. J. Hydrogen Energy* **2023**, *48*, 12519–12522. [CrossRef]
105. Xiang, P.; Liu, J.; Zhao, W.; Ji, Q.; Ao, C.; Wang, X.; Sun, P.; Wang, X.; Li, Z. Experimental investigation on gas emission characteristics of ammonia/diesel dual-fuel engine equipped with DOC + SCR aftertreatment. *Fuel* **2024**, *359*, 130496. [CrossRef]
106. Tyrewala, D.; Prikhodko, V.; Kaul, B.; Curran, S. Simultaneous control of unburned NH3 and NOx emissions from high load dual-fuel ammonia operation on a high-speed diesel engine using a Cu-SCR system. *J. Eng. Gas Turbines Power* **2026**, *148*, 031016.
107. Wu, M.; Cova-Bonillo, A.J.; Gabana, P.; Brinklow, G.; Khedkar, N.D.; Herreros, J.M.; Rezaei, S.Z.; Tsolakis, A.; Millington, P.; Clave, S.A.; et al. Addressing the challenge of ammonia slip and nitrous oxide emissions from zero-carbon fuelled engines through catalytic aftertreatment solutions. *Int. J. Hydrogen Energy* **2024**, *94*, 848–861. [CrossRef]
108. Sun, X.; Wang, H.; Xu, Z.; Wang, Y.; Wang, X.; Liu, J. Nitrogen oxides and ammonia removal analysis based on three-dimensional ammonia-diesel dual fuel engine coupled with one-dimensional SCR model. *Energies* **2023**, *16*, 908. [CrossRef]
109. Ghosh, R.S.; Le, T.T.; Terlier, T.; Rimer, J.D.; Harold, M.P.; Wang, D. Enhanced selective oxidation of ammonia in a Pt/Al_2O_3@Cu/ZSM-5 core–shell catalyst. *ACS Catal.* **2020**, *10*, 3604–3617. [CrossRef]

110. Yao, D.; Li, Y.; Wu, F.; Jin, W.; Zhang, Z.; Hu, X.; Hu, J. Modeling and analysis of ammonia oxidation and nitrous oxide formation on a dual-layer ammonia slip catalyst for diesel after-treatment. *React. Chem. Eng.* **2023**, *8*, 2040–2051. [CrossRef]
111. Brandenberger, S.; Kröcher, O.; Tissler, A.; Althoff, R. The state of the art in selective catalytic reduction of NOx by ammonia using metal-exchanged zeolite catalysts. *Catal. Rev.* **2008**, *50*, 492–531. [CrossRef]
112. Jabłońska, M. Review of the application of Cu-containing SSZ-13 in NH_3-SCR-DeNO_x and NH_3-SCO. *RSC Adv.* **2022**, *12*, 25240–25261. [CrossRef] [PubMed]

https://doi.org/10.3390/en19143357